Spatial MILP optimization framework for siting Hydrogen Refueling Stations in heavy-duty freight transport

International Journal of Hydrogen Energy 94 (2024) 669–686

Contents lists available at ScienceDirect

International Journal of Hydrogen Energy

journal homepage: www.elsevier.com/locate/he

# Spatial MILP optimization framework for siting Hydrogen Refueling Stations in heavy-duty freight transport

Antonio De Padova [a,b,*], Daniele Salvatore Schiera [a,b], Francesco Demetrio Minuto [a,b], Andrea Lanzini [a,b]

[a] Department of Energy, Politecnico di Torino, Corso Duca degli Abruzzi 24, 10129, Torino, Italy
[b] Energy Center Lab, Politecnico di Torino, Via Paolo Borsellino 38/16, 10138, Torino, Italy

ARTICLE INFO

Handling Editor: Prof. A.B. Basile

*Keywords:*
Hydrogen refueling station
Heavy-duty transport
Hydrogen trucks
Normative constraint
Geospatial analysis
Graph optimization

ABSTRACT

The need for deep decarbonization of the transport sector cannot be understated, as it accounts for about the 25% of greenhouse gas emissions in Europe. Developing hydrogen-based trucks is one of the viable solutions for exploiting green hydrogen and reaching climate neutrality. This work presents an optimization framework to optimally place Hydrogen Refueling Stations (HRS) for hydrogen-based trucks under technical, policy and regulatory constraints. It relies on an EU heavy-duty road freight transport database adapted to the latest publicly available statistics to update the demand intensity. A revised Node Capacitated Flow Refueling Location Model is proposed to minimize the number of HRS to be sited on the highway network. The node capacity constraint considers standard sized HRS with a maximum daily capacity ranging from 500 (S-sized) to 4000 kg (XL-sized). The framework can be a useful evaluation tool to strategically site HRS, both for policymakers and stakeholders. To this end, the Italian highway network was evaluated as a case study, finding that at least 78 HRS nodes are required across the road network if a 10% share of hydrogen vehicles is considered, as planned in the Italian National Recovery and Resilience Plan. The median utilization factor of the refueling stations is 67.5%, ranging from 49% for the S-sized to 86% for the XL-sized, which are located mainly in northern Italian regions. To effectively reduce emissions in road freight transport, results show that at least 368 MW of additional equivalent photovoltaic capacity is needed to produce entirely green hydrogen, reducing the greenhouse gases emissions associated to the road freight transport by 6.5%.

## 1. Introduction

### 1.1. Background and motivation

The European Green Deal outlines an ambitious goal for the European Union (EU) to achieve climate neutrality by 2050. In detail, it aims to reduce emissions in the transport sector by 90% by 2050 [1]. It is worthwhile to mention that in 2019 the transport sector accounted for almost 25% of greenhouse gases (GHG) emissions across Europe [2]. While heavy-duty (HD) vehicles represent less than 2% of the overall circulating vehicles in Europe [3], they account for approximately 27% of $CO_2$ emissions of the whole road transport sector and about 6% of all GHG emissions in the EU [4]. Furthermore, among the various categories of HD vehicles, trucks are responsible for about 85% of these emissions [5]. This highlights the urgent need for decisive action on the freight transport segment to address the environmental impact of the whole sector.

The transition to low- or zero-emission vehicles, based on alternative powertrains, is therefore essential to achieve the stringent targets set by the EU. Despite having a high efficiency, Battery Electric Vehicles (BEVs), which are the most promising and adopted solution for the decarbonization of the light-duty transport sector, have both low power as well as energy density, so they face significant limitations in payload and range [6,7]. Moreover, considering the high battery recharging times and the impacts these limitations have on transport operations, they do not seem a viable solution in the short term for the long-haul freight transport segment. Long-haul transport is thus considered a hard-to-abate sector, and alternative powertrain solutions should be further investigated.

In comparison to BEVs, Fuel Cell Hydrogen Electric Vehicles (FCHEVs) offer longer driving ranges on a single charge. They also have a payload capacity comparable to traditional diesel vehicles and feature

* Corresponding author. Department of Energy, Politecnico di Torino, Corso Duca degli Abruzzi 24, 10129, Torino, Italy.
*E-mail address:* antonio.depadova@polito.it (A. De Padova).

https://doi.org/10.1016/j.ijhydene.2024.11.086
Received 23 July 2024; Received in revised form 23 October 2024; Accepted 4 November 2024

short refueling times [8,9]. On this aspect, since the EU Regulation 561/2006 [10] sets limitations on the daily driving time and imposes 45 min pause every 4.5 h or, alternatively, two breaks of 15 and 30 min respectively during the 4.5 driving hours, it is important to have refueling times compatible with such mandatory stops to avoid unnecessary wastes of time. Also, in case of a higher energy need (e.g., for refrigerated equipment, on-board air conditioning or cabin heating), FCHEVs can provide additional energy without drawbacks for payload capacity. Therefore, FCHEVs could represent a promising solution to reduce GHG emissions in mid or long-haul applications [11], while resulting in a competitive Total Cost of Ownership (TCO), since the capital costs of the main components is expected to decrease significantly in the next years [12,13]. However, a publicly accessible and conveniently distributed refueling infrastructure is a key condition to enhance a widespread adoption of FCHEVs.

By the summer of 2023, as observed by the Clean Hydrogen Partnership [14], there were 178 operational and publicly accessible Hydrogen Refueling Stations (HRS) [15] across Europe. Most of them (96) are in Germany, while only 1 is in Italy. In response to the NextGen EU, which explicitly targets the acceleration towards the use of sustainable transport and thus the deployment of charging and alternative refueling stations, Italy proposed its own National Recovery and Resilience Plan (NRRP), in which 230 M€ have been allocated to 'Investment 3.3 - Hydrogen Experimentation for Road Transport', with the aim to install 40 HRS on its territory. The plan forecasts a penetration rate of 5–7% by 2030 for FCHEVs in the HD segment [16]. The HRS infrastructure deployment is a classic "chicken and egg" dilemma since high investment costs are required and low utilization is expected at the beginning [17], thus making essential to develop proper design and dimensioning methodologies to accelerate the diffusion of these vehicles.

### 1.2. Literature review

Over the last decades, several methods have been proposed to optimally locate e-fuels refueling stations. Facility location models, which are optimization problems, are used to determine a set of locations required to satisfy the user demands within a network [18,19]. These models aid in addressing the placement problem by providing preliminary suggestions for the optimal locations of HRS based on specific objective function, such as minimizing the overall investment cost or the number of facilities. The two most popular approaches are node-based and path-based demand models.

In the node-based methods, the demand is expressed at fixed points in a network and the facilities are properly located to fulfil it. They usually rely on registry data (i.e., population, vehicle registrations, etc.) to calculate the demand in each network node. Covering, p-median and p-center models are the most relevant examples of this approach. The first type, "Covering models", can be further classified as set-covering models, when they evaluate the minimum number of facilities needed to satisfy all the demand nodes [20,21], or maximal-covering-location models, if they maximize the demand covered by a given number of stations [22,23]. Gündüz et al. [24] investigated the problem of locating HRS in Istanbul, with a modified version of the set covering model in which real distances data are used instead of Euclidean distance. The *p*-median model optimizes the location of a given number ($p$) of stations assigning them demand nodes by minimizing the average distance that is travelled from a demand node to all the located facilities [25]. Several adaptions of this model have been used, considering other "costs" instead of distance (e.g., the driving time) [26]. Kim et al. [27] proposed a HRS deployment plan for Korea by using three mathematical models. With the first, the demand estimation module, they determined the required number of refueling stations to satisfy the target covering ratio of the total demand and, for the given number of stations, maximal-covering and *p*-median models are used sequentially to place the hubs and to allocate the demand to them. The *p*-center model, instead, reduces the maximum distance between a node and the station that covers its demand [28]. However, these models typically consider a costumer behavior which consists in refueling close to home (or, in general, to the demand node), mainly with dedicated trips.

In path-based demand models the demand in a network is associated with traffic flows from an origin to a destination. This is the case of the so-called Flow Intercepting Location Models. These kinds of models are particularly suitable for our study because, in the context of freight transport, refueling typically occurs during regular daily operational routes rather than on dedicated trips. In 1990, Hodgson proposed the Flow Capturing Location Model (FCLM) [29], which considers traffic in a network as a demand flow. The origin-destination (O-D) trip follows a path along multiple nodes, which are candidate facilities location. The model maximizes the captured flow by a given number of facilities. By combining the FCLM with a greedy algorithm, Hodgson et al. located hydrogen stations in Canada, using the peak-hour traffic flow in the morning to simulate the all-day traffic flow [30]. Shukla et al. [31] slightly modified the FCLM by introducing a budget constraint on the overall number of facilities and applied it to the transportation network of Alexandria, Virginia. Li et al. [32] proposed an integration between a generalized Bass diffusion model and the FCLM to explore the mutual interaction between vehicle sales and the number of refueling stations and thus to make a long term location plan. Honma and Kuby [33] compared the FCLM and a *p*-median model, by defining upper limits on vehicle driving range and maximum inconvenience on refueling trips, finding that path-based approach results in less stations to cover an urban area, as they assume that residents of a zone interact with other urban zones during their daily routes. However, these models assume that if a facility is located along a flow's path, i.e., if the traffic flow intercepts a facility, the demand is covered and satisfied. This assumption does not consider the limited range of vehicles, so that it may be necessary to stop multiple times along a journey to reach the destination, which is particularly relevant in long-haul transport sector. Kuby and Lim dealt with this limitation developing the Flow Refueling Location Model (FRLM), which optimally locates $p$ refueling stations on a network to maximize the total flow volume refueled. They proposed both a nodes-only version of the problem, in which the candidate sites of the facilities are only the nodes of the network [34], and an extension in which candidate sites are added along arcs too [35]. In their works, they proposed a two-stage approach that uses pre-generated viable combinations of possible refueling stations for each path, taking into account the vehicle limited driving range. MirHassani and Ebrazi [36] re-formulated the FRLM presenting a flexible MILP model, eliminating the need for pre-generating facility combinations. This formulation allowed to obtain an optimal solution much faster than the previous versions and to be solved in the maximum cover form too. Kim and Kuby [37] presented the deviation-flow refueling location model (D-FRLM), in which they relaxed the basic FRLM to consider the willingness of consumers to deviate from their shortest paths to reach a service facility. Jochem et al. [38] applied the FRLM model to the German highways and further extended it by including the specific access distances for each rural district (origin or destination) to the closest highway driveway and exit, since the whole trip distance is relevant for the demand for recharging and not only the mileage travelled on the highway. These authors, however, assumed each station with unlimited daily fuel capacity, which may not be a realistic assumption. Upchurch et al. [39] introduced the capacitated flow refueling location model, that limits the amount of flow that any facility can refuel. However, they stated that "the amount of refueling capacity that could be built at each node is potentially infinite", meaning that multiple facilities could be built at a single node. Furthermore, they showed how locations that were optimal for the uncapacitated FRLM may be suboptimal for the capacitated one. Staněk et al. [40] also assessed this limitation and they extended the deterministic FRLM by considering a limited capacity of charging stations and location-dependent construction costs for the location and dimensioning of electric vehicles charging infrastructure. However, in

their model it is not possible to split the flow volume of a certain path such that different flow proportions use different sequences of charging stations. This feature is included in the model proposed by Rose et al. [41], where the capacity limitation is not given by the single station capacity, but by the limited capacity of the candidate sites (i.e., network nodes), and the objective is to minimize the total number of facilities to serve the 100% of the traffic flow. They applied their model to the case study of a potential FCHEVs refueling infrastructure in Germany and the location capacity limit was found to have a significant impact on the number of stations required. They further extended their research, by combining the capacitated FRLM and an electricity system optimization model that takes grid expansion options into account [42] and by introducing new constraints to assess hydrogen supply options and to determine the associated costs in two different delivery scenarios [43]. However, they considered the vehicle's maximum achievable range with a single charge, i.e., vehicle autonomy, as the only constraint on the distance between each stop. Since other restrictions could be set by the legislation, as in the case of EU Regulation 561/2006, they should be considered too. In particular, the normative limit is a bottleneck, being usually shorter than the vehicle autonomy. Furthermore, they properly argued that the refueling amount varies at each node depending on the total distance and the distance of the node from the starting point. Nevertheless, it is worth noting that, in case of multiple stops, it also depends on where the previous refueling stops occurred. Finally, they used a fixed value for the initial vehicle range parameter.

### 1.3. Paper contribution

By considering the abovementioned literature, this work proposes a new methodological approach to deal with the main limitations that have been highlighted, improving the optimal stations siting in a network. First, the optimization model has been re-formulated and adapted to a different type of input data. Indeed, in the pre-processing step for each path the possible refueling strategies with the minimum number of stops are pre-determined, also by considering normative limitations. This new approach allows to determine the actual number of refueling stops needed during a trip, which in the existing literature is computed as the ratio between the travelled distance and the maximum vehicle range. It has been found that this latter definition may lead to infeasibilities of the problem solution in some circumstances (e.g., when a single stop is theoretically sufficient, but there is no free space enough in the tank at any node to refuel what it is needed). Moreover, the proposed methodology evaluates the precise fuel amount eventually required on each node of the network, also depending on where previous stops occurred. An incorrect assessment of this quantity may lead to over-estimate the total demand on a node, and thus to exceed the daily capacity limitation and eventually to install a further hub. A novelty has also been introduced in the network topology definition. The position of starting and ending nodes of each path is defined by considering the specific land use of the territory, while in other works it is represented simply as the geometric centroid of the latter. In this way, a slightly better estimation of the actual travelled distance is achieved, as it is discussed in Section 2.2.2. Moreover, with respect to previous works, we provide a valuable sensitivity analysis on the initial vehicle range parameter, finding that it may have a significant impact on the number of required stations (as deepen in Section 3.2). Finally, the framework has been applied to optimally dimension a hydrogen refueling infrastructure for HD vehicles optimally on the Italian territory and compared with the development plan of the Italian NRRP.

### 1.4. Outline of the paper

In Section 2, the methodology of the framework is presented. It is articulated in three main steps, which are analyzed in depth each in a dedicated paragraph. Section 2.1 lists some general assumptions on which the framework is based. Section 2.2 then describes the raw data handling step, with the definition of the origin-destination input matrix and the characterization of the network topology. In section 2.3 the input data pre-processing step is described, with the definition of the refueling strategies which serve as input of the proposed optimization model that is finally described in section 2.4. Sections 2.5 and 2.6 present the Italian case study specific assumptions and three different $CO_2$ emissions' scenarios, respectively. In section 3 the main findings of the study are highlighted, presenting a possible optimal Italian HRS network configuration (section 3.1) and evaluating the carbon emissions reduction performances in the three scenarios (section 3.2). A sensitivity analysis is then performed on the initial vehicle range parameter (section 3.3). In section 4 the main results are discussed and compared with the findings of another study and with the announced development plan of the Italian infrastructure based on the policy funding scheme. Furthermore, the model main limitations are presented. Finally, in section 5, together with the final considerations, the recommendations for future developments are listed.

## 2. Materials and methods

The framework proposed is based on a node-capacitated flow refueling location model (NC-FRLM), incorporating normative constraints together with vehicles' technical limitations and georeferenced data. The hydrogen demand across the network is associated to the traffic flow, and it must be satisfied along a path from an origin to a destination (O-D path). Each origin-destination is represented as an ordered succession of network nodes. The framework has the aim of minimizing the total number of HRS to refuel all the vehicles travelling through the network and to allow them to reach their destination.

The framework is articulated in three main parts, as highlighted in Fig. 1: raw input data handling step (Section 2.2), data pre-processing step (Section 2.3) and optimization model (Section 2.4). In the first part the raw data are taken from different publicly available sources and elaborated to have a O-D matrix which serves as input data. It is further handled by generating, for each O-D path, the set with the all the possible refueling strategies and with the fuel amount needed on each node depending on the adopted refueling strategy. Finally, these two sets represent the actual input data for the optimization model, which minimizes the overall number of HRS to be placed on the network. For the sake of clarity, the methodology is explained through the example of Italian regions. Nevertheless, it is worth nothing that the framework could be used for any European country for which the same statistical data are available.

### 2.1. General assumptions

Before getting into the main steps of the proposed framework, this section outlines the general simplifying assumptions, which are referred to three main fields: the O-D paths, the vehicles and their drivers, and the hydrogen refueling stations' locations.

#### 2.1.1. Origin-destination paths

To reference countries' regions for statistical purposes, the EU has developed a classification known as Nomenclature of territorial units for statistics (NUTS), subdividing the economic territory of the EU into regions at three different levels (NUTS-1, NUTS-2 and NUTS-3, moving from larger to smaller territorial units) [44]. Every origin-destination path is assumed to start from a representative point within the origin NUTS-3 region and end at a representative point within the destination NUTS-3 region, referred to as NUTS-3 nodes. Intra-regional trips (i.e., within the borders of the same NUTS-3 region) are not considered. Since NUTS-3 nodes may not be located on the main road network, a virtual road is added to connect the NUTS-3 nodes and the main road network, based on the shortest linear distance among them (detailed in section 2.2.2). Based on these assumptions, a O-D path is defined as the shortest path from the origin to the destination point on the road network. It is

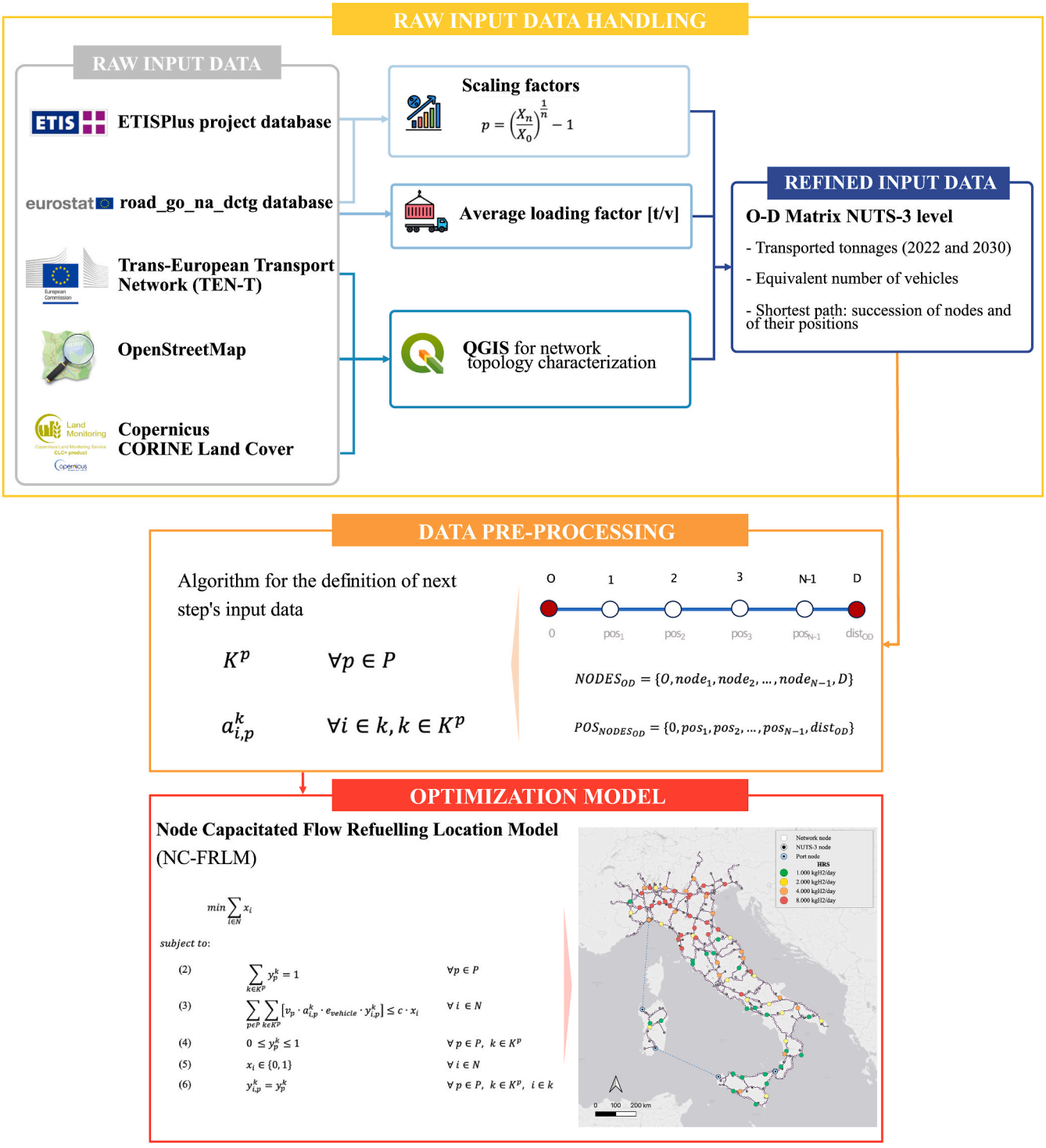


**Fig. 1.** Summary diagram of the framework.

important to note that the O-D path is a set of ordered succession of points along the road network, representing a vehicle trip of a certain length ($dist_{OD}$). The daily traffic volume on each O-D path is known in advance and it is assumed to remain constant throughout the year.

### 2.1.2. Vehicles and drivers

Some simplifying assumptions are made regarding the technical specifications of the vehicles, due to the wide range of declared autonomies by different manufacturers and the pre-commercial state of this technology. It is thus assumed that all vehicles have the same technical specifications, meaning they have the same maximum achievable range ($VR_{max}$) and fuel consumption rate ($e_{vehicle}$, expressed in $kg_{H_2} \cdot km^{-1}$). The $e_{vehicle}$ is assumed to be proportional only to the travelled distance, thus, neglecting the possible effects of road grade, driving behavior, idling, vehicle weight, and other parameters [45,46] for simplicity. For the sake of clarity, since it is assumed that the vehicle's fuel consumption rate depends only on the travelled distance, the fuel quantities will be referred to in terms of equivalent achievable range, and therefore in kilometers as unit of measure.

Each vehicle starts with a certain initial vehicle range ($VR_i$) and ends

its trip with the same fuel level, meaning the residual vehicle range ($VR_f$) at the end of the route is equal to $VR_i$. Therefore, each vehicle refuels along its path exactly a fuel amount corresponding to $dist_{OD}$. This constraint assures that the whole fuel demand is completely met using the refueling infrastructure on the main road network, rather than at the urban NUTS-3 nodes locations. This assumption is useful to represent the actual daily energy requirement for the routes and ensures that each vehicle could eventually reach any destination from any origin. Additionally, recent European national freight road transport data show that approximately 74% of the goods are transported in "hire and reward" mode (for Italy, almost 87%). This means that trucks, which are operated by third parties transport providers, may receive new delivery order to different locations once they reach their destinations [47].

As the framework is applied to freight transport, it is assumed that the trucks drivers are fully aware of the location of the HRS along their routes and refuel efficiently to complete their trip according to a refueling strategy which is pre-assigned to them by their logistic fleet operator. If multiple stops ($S_p$) are required, it is assumed that for the first $S_p - 1$ stops, the tank is filled to its maximum capacity.

Each trip is assumed to be completed in one single day. According to Regulation (EC) No. 561/2006, which imposes a maximum daily driving time of 9 h and a 45-min break every 4.5 h of driving (or two breaks of 15 and 30 min, respectively, during the 4.5-h driving period), the following assumptions are made.

- Paths with distance ($dist_{OD}$) of less than 720 km (considered the maximum daily distance that can be travelled by a single operator at a speed of 80 km $km{\cdot}h^{-1}$) are completed by a single driver.
- Paths with a distance of more than 720 km are completed by two operators.

For paths with $dist_{OD} \leq 720$ km, the maximum driving distance between each stop ($dist_{max}$) is limited to 360 km (4.5 h at 80 $km{\cdot}h^{-1}$) and not by the $VR_{max}$. For paths with $dist_{OD} > 720$ km, $dist_{max}$ is equal to $VR_{max}$, as the two operators can take their mandatory rest periods while the other is driving.

#### 2.1.3. Hydrogen refueling stations

HRS share similar safety and space requirements with conventional fuel stations [48]. Thus, it is reasonable to expect that HRS will be constructed jointly with conventional fuel stations or by reconverting some of them. It is assumed that stations can only be located at network nodes representing the centroids of existing service and refueling areas in the network. Consequently, stations cannot be located at intersection points, road networks entries or exits, or at the NUTS-3 nodes. Both HRS and nodes have capacity limitation on the amount of fuel they can dispense daily. Since a node is assumed to capture traffic flow in both directions, the node capacity is twice that of a single HRS. In other words, it is assumed that each node will have two stations, one for each travel direction. This assumption is supported by the fact that refueling stations on highways often constructed in pairs, with one station on each side serving traffic in opposite directions. For simplicity, we represented the actual fuel demand on each node as the sum of the fuel demands from vehicles travelling in both directions. However, this approach does not account for potential differences in traffic flow between directions, which could result in the two stations requiring different capacities.

### 2.2. Raw input data handling

In this step, raw input data are gathered from several publicly accessible sources and processed to create an updated O-D input matrix, which includes all considered O-D paths. The following sections explain more in detail how statistical data and a previous O-D matrix are used to characterize the vehicles traffic flow on each path. Additionally, georeferenced data are used to determine the network topology on which these paths actually occur. In this work, the Italian main road infrastructure will be used to illustrate the proposed methodology.

#### 2.2.1. Vehicle traffic flows

The data regarding the traffic flow on each O-D path are based on the results of the European Transport Polity Information System (ETIS-BASE) [49], which has been further extended in the ETISplus project [50]. One of the main outputs of these studies was an O-D matrix representing the transported goods volumes between the NUTS-3 European regions for the year 2010, in the most recent version of the database.

Only the national road freight transport, defined as road transport between two places located in the same country by a vehicle registered in that country, has been considered in our study, as it constitutes around the 97% of the tons transported in Italy [51]. Only the paths with Italian NUTS-3 regions as both the starting and ending regions have thus been selected and considered.

The data contained in the ETISplus Road Freight Matrix, which refers to the year 2010, have been scaled to the most recent publicly available statistics (year 2022), reported by Eurostat in the *road_go_na_dctg database*. This database contains national road freight transport statistics by distance class, type of goods and type of transport. To achieve this adaptation, the approach used by Speth et al. [52] has been employed and further adapted. Three different scaling factors have been defined and used, depending on the distance class. From 2010 to 2022, the transported goods over different distance classes did not vary at the same rate, as reported in Table 1.

- Transport over shorter distances (<150 km) decreased more significantly,
- Transport over medium (150–500 km) and long distances (>500 km) remained almost the same [53].

The scaling factor for each distance class for the tons transported from the year 0 to the year 0+n is defined as a Compound Annual Growth Rate (CAGR) expressed by the following equation:

$$f_{scale,dist\ class} = \left(\frac{X_{0+n,dist\ class}}{X_{0,dist\ class}}\right)^{\frac{1}{n}} - 1$$

where $X$ is the measured data for the aggregated volume of goods transported in Italy for each distance class, at year 0 and $0 + n$.

Once the scaling factors are defined, the tons transported on each route are scaled to 2022 and to 2030 with:

$$X_{path,2022} = \left(1 + f_{scale,dist\ class,p}\right)^{12} \cdot X_{path,ETIS\ 2010}$$

$$X_{path,2030} = \left(1 + f_{scale,dist\ class,p}\right)^{8} \cdot X_{path,2022}$$

where $X_{path,ETIS\ 2010}$ is data for the aggregated volume of goods transported on each path reported by ETISplus for the year 2010, and $X_{path,2022}$ and $X_{path,2030}$ the estimated values for the years 2022 and 2030 respectively.

Finally, an average loading factor $F_{load}$ of 15.7 tons per vehicle has been calculated for the years from 2010 to 2022 to convert the transported tons in equivalent vehicles carrying them. Furthermore, since Eurostat reports that almost the 25% of the total national road freight transport performance (in vehicle-kilometers) in the EU is carried out by

**Table 1**
Scaling factors by distance class.

| | <150 km | 150–500 km | >500 km |
|---|---|---|---|
| $X_{2010}$ [1000 t] | 1154225 | 285890 | 47322 |
| $X_{2022}$ [1000 t] | 706145 | 266075 | 43995 |
| $f_{scale,dist\ class}$ | **−4.01%** | **−0.60%** | **−0.61%** |

empty vehicles, the number of vehicles is divided by a factor of 0.75 to take into account the share of empty runs ($S_{empty\ runs}$). As these data are not available for Italy, the average EU value has been used. The equivalent number of vehicles running along each path is thus calculated as:

$$v_p = \frac{X_{path,year}}{F_{load} \cdot (1 - S_{empty\ runs})} = \frac{X_{path,year}}{15.7 \cdot 0.75}$$

### 2.2.2. Network topology definition

The network used in this work is constituted mainly by three elements: the NUTS-3 nodes, the network nodes, and the links among them.

The origin and destination nodes are defined as the weighted centers of the origin-destination NUTS-3 Italian regions. These centers are obtained by weighting five of the 44 thematic classes from the CORINE Land Cover (CLC) Italian dataset, which provides a land cover and land use inventory with a minimum mapping unit of 25 ha (ha) [54]. The selected attributes (i.e., continuous and discontinuous urban fabric area, industrial or commercial units, port areas, roads, rails and associated lands) have different weights depending on their expected importance in the transport sector. In particular, continuous urban fabric refers to urban areas where 80% or more of the land is covered by urban development (such as buildings, roads and other infrastructure), with the remainder being open spaces or small patches of unveloped land. This excludes bodies of water. In discontinuous urban fabric, on the other hand, the land coverage corresponds to 30–80%.

As illustrated in Fig. 2, the use of weighted centroids (green circle) shifts the center closer to significant areas of the region, such as industrial or commercial hubs, while the geometric centroid (orange square) may end up in less relevant locations, such as the sea or areas with minimal productive or transport activity. This approach provides a more accurate estimate of the actual distance travelled from the origin node, the main road network, and the destination node. In Fig. 2, for example, the geometric centroid is located in the sea near Venice, whereas the weighted centroid is placed on land, closer to areas of commercial interest.

With the Regulations (EU) 1315/2013 and (EU) 1316/2013, the European Commission defined a fully operational, multimodal Trans-European Transport Network (TEN-T) for a sustainable and smart transport. TEN-T network is defined on three levels: 9 core network corridors, the core network and the comprehensive network [55]. In this work, the TEN-T network has been used as road network for the national road freight transport system.

As already mentioned, HRS candidate sites (network nodes) are defined as the centroids of existing service or refueling areas in the network. The GIS-data concerning the operative fuel distributors and rest or services areas throughout Italy have been retrieved by means of an Overpass API on OpenStreetMap.

Both the TEN-T network and the refueling stations dataset are processed using the free open-source geographic information system software, QGIS [56]. The conventional fuel stations are represented as a point layer, while the network is a line layer. First, only the points within a buffer distance of 500 m from the road line are selected (node filtering, Fig. 3a). This buffer distance serves as a tolerance to account for potential inaccuracies in the location of fuel stations and rest areas along the TEN-T road network. Next, a buffer area with a radius of 3 km is created around the filtered nodes. This buffer size was chosen after testing various distances, ranging from 1 to 5 km, to achieve a balance between having a sufficiently populated network and reducing the computational complexity of finding the optimization solution. The centroids of these dissolved buffer areas are obtained and used as network nodes, thus actually identifying potential representative areas and not a precise and punctual locality where HRS could be located (network nodes definition, Fig. 3b).

Additional nodes are manually added at road intersections and at the

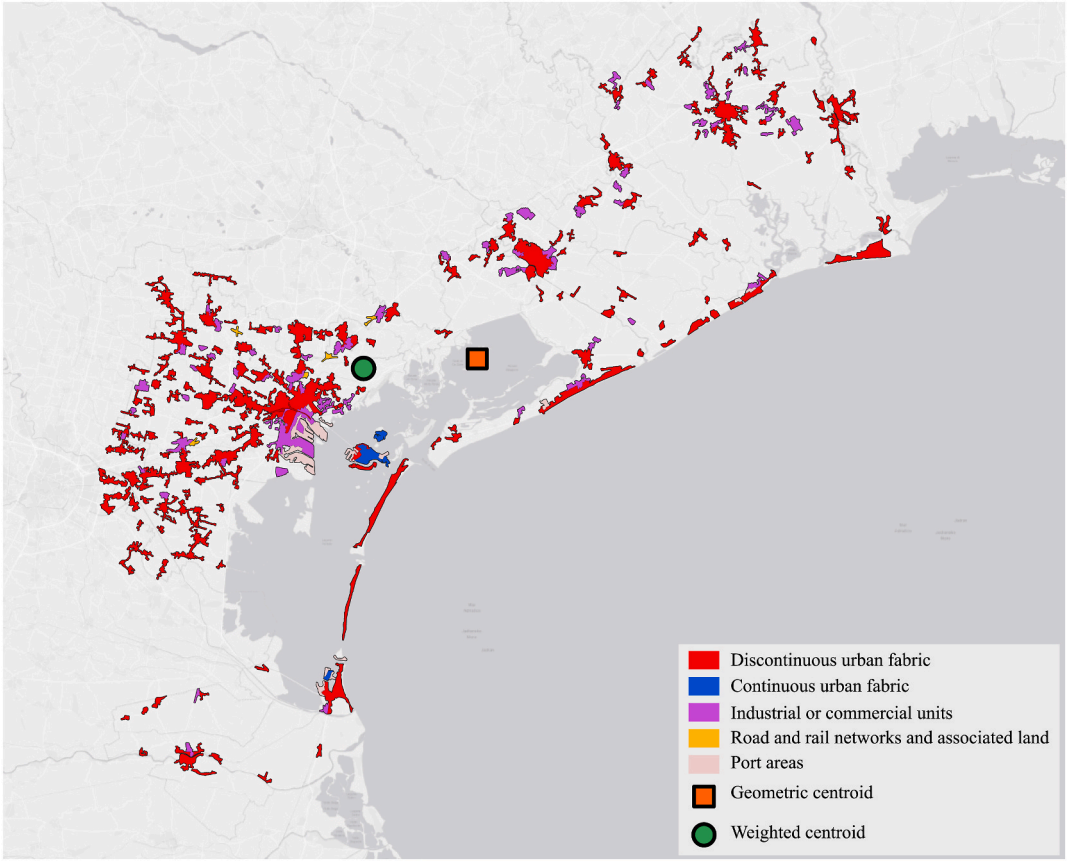


**Fig. 2.** – Geometric centroid and weighted centroid of an Italian NUTS-3 region (Venice).

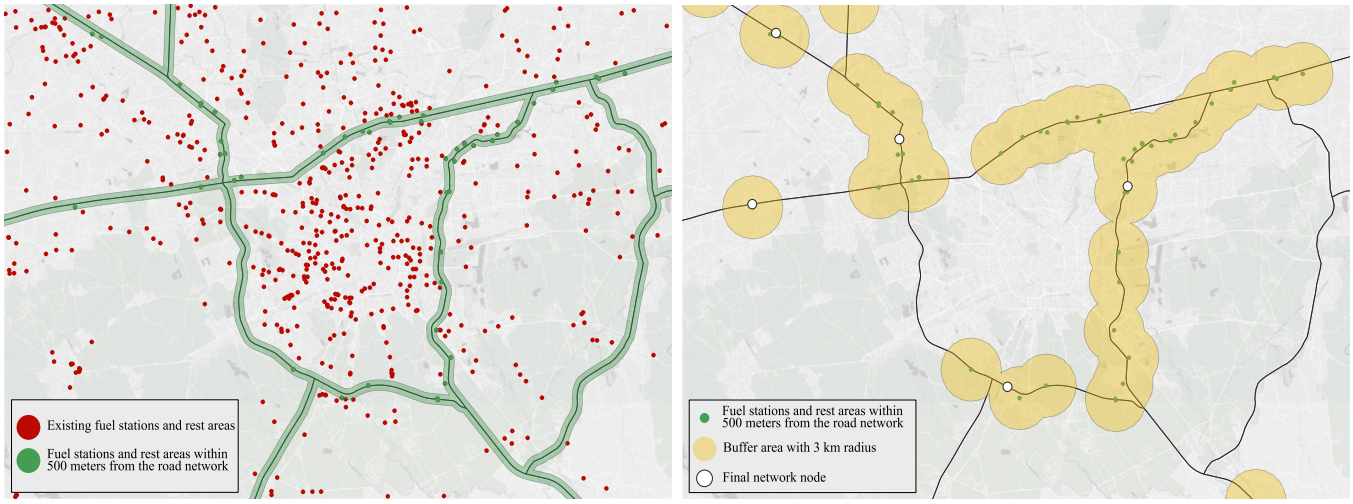


**Fig. 3.** Example of (a) node filtering and (b) network nodes definition near the city of Milan.

identified entries and exits of the main road network. At the end of this process, the network consists of.

- 107 NUTS-3 nodes (or O-D nodes),
- 590 fuel areas centroids,
- 162 intersection nodes,
- 107 main road entrances and exits,
- 6 port nodes,
- 944 main road network edges,
- 107 virtual distances from origin/destination to main road,
- 3 ferry edges.

All the edges connecting two ports (i.e., distances travelled by ferry) are considered to have no impact on the fuel consumption and are therefore considered with a "road length" equal to 0 km.

Finally, the shortest path from the origin node to the destination node is calculated by using the QGIS function "shortest path from point to point", which is built on the Dijkstra algorithm [57]. As represented in Fig. 4 with an example, each O-D path is thus represented by two vectors.

- An ordered succession of nodes along the main road network
- A list with the position of each node with respect to the origin of the path (*pos*), in kilometers.

The network nodes and edges used to represent the network are reported in the open source database [58], together with the O-D path matrix.

### 2.3. Data pre-processing

In this step of the methodology, possible refueling strategies for each path are determined. These strategies include all combinations of nodes along the path that allow completing the route with the fewest possible stops, while ensuring that $VR_f$ equals $VR_i$.

The data pre-processing step is illustrated in Fig. 5 with its flowchart. First, $dist_{max}$ and the driving range before the first stop ($1stStopRange$) must be defined based on the path's characteristics, as follows:

- if $dist_{OD} \leq 720$ km, $dist_{max}$ is limited to 360 km,
- if $dist_{OD} > 720$ km, $dist_{max}$ is imposed equal to $VR_{max}$,
- $1stStopRange$ is the minimum between $VR_i$ and $dist_{max}$ for both the cases.

The minimum number of stops for each path $p$ ($S_p$) is then determined with an iterative process. The initial value of $S_p$ is set to 1 and an array, $\mathbb{S}_1$, is populated with the $M$ nodes whose position with respect to the origin ($pos_{node}$) is within the range (0, $1stStopRange$]. For each $m$-th node of the $\mathbb{S}_1$ array, the vehicle tank availability ($r_{m,\mathbb{S}_1}$) can be evaluated. It is the amount of free space available in the vehicle's tank at that node with position from the origin $pos_{m,\mathbb{S}_1}$ (or, in other words, the complement to a full tank in that node) and can be calculated as:

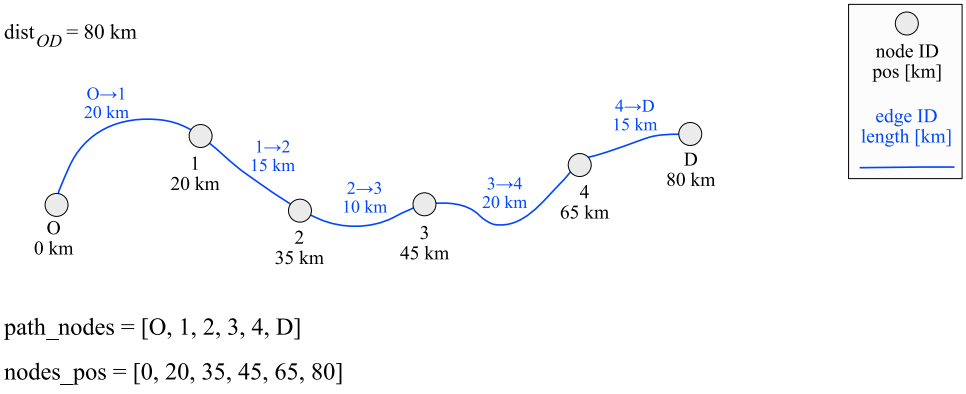


**Fig. 4.** Example of O-D path.

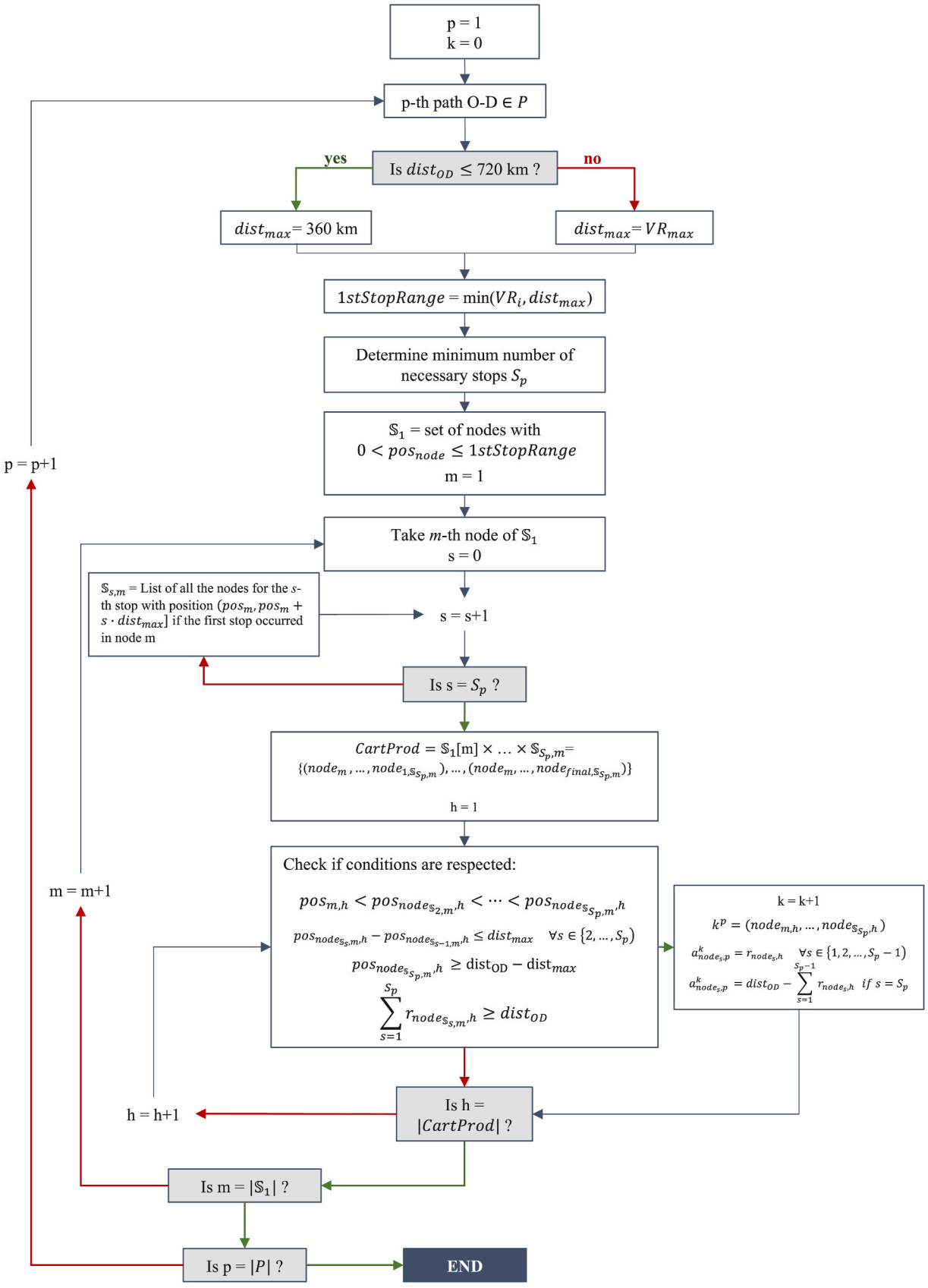


**Fig. 5.** – Flowchart of the data pre-processing step.

$$r_{m,\mathbb{S}_1} = VR_{max} - \left(VR_i - pos_{m,\mathbb{S}_1}\right) \quad \forall m \in \{1,2,..,M\}$$

If at least one of these nodes has $r_{m,\mathbb{S}_1} \geq dist_{OD}$ and it is not farther than $dist_{max}$ from the destination, only one stop would be needed to complete the trip, and the process stops here. If not, $S_p$ is increased by 1. A new set $\mathbb{S}_{S_p}$ is defined, with all the nodes in the range $(pos_{M,\mathbb{S}_1}, pos_{M,\mathbb{S}_1} + (S_p - 1)\cdot dist_{max}]$. The last element of this set represents the farthest node reachable for the $S_p$-th stop after the first stop occurred in the M-th node of $\mathbb{S}_1$. Assuming that the tank is filled to its maximum for the first $S_p - 1$ stops, the tank availability at the final node of $\mathbb{S}_{S_p}$ set is equal to:

$$r_{final,\mathbb{S}_{Sp}} = pos_{final,\mathbb{S}_{Sp}} - pos_{final,\mathbb{S}_{Sp-1}}$$

with the pedis *final* referring to the last node of set $\mathbb{S}_{S_p}$ and being equal to $M$ if $S_P - 1$ is equal to 1. This process is repeated iteratively until the following condition is met:

$$\sum_{s=1}^{S_p} r_{final,\mathbb{S}_s} \geq dist_{OD}$$

where $r_{final,\mathbb{S}_s}$ is the tank availability in the last node of the $s$-th stop nodes set.

Once the minimum number of stops is determined, the refueling strategies can be defined. If $S_p = 1$, only nodes with $r_{m,\mathbb{S}_1} \geq dist_{OD}$ and a position within $dist_{OD} - dist_{max}$ and $dist_{OD}$ are considered as possible refueling strategies, and the amount of fuel refueled at these nodes is equal to $dist_{OD}$. For all other cases, for each $m$-th node in $\mathbb{S}_1$, other $S_p - 1$ arrays are generated: the first array includes all the nodes in the range $(pos_m, pos_m + dist_{max}]$, the second set includes all the nodes in the range $(pos_m, pos_m + 2\cdot dist_{max}]$, and so on, until the last set is generated with nodes in the range $(pos_m, pos_m + (S_p - 1)\cdot dist_{max}]$. Then, a cartesian product among them is performed, creating combinations of $S_p$ nodes. Only the combinations with $pos_m < pos_{node,\mathbb{S}_{2,m}} < \ldots < pos_{node,\mathbb{S}_{Sp,m}}$, with a distance among them less than or equal to $dist_{max}$, and with $pos_{node,\mathbb{S}_{Sp,m}} \geq dist_{OD} - dist_{max}$ are considered. Finally, the $h$-th combination is considered as an effective refueling strategy for the path $p$ ($k^p$) only if the following condition is realized:

$$\sum_{s=1}^{S_p} r_{node_s,h} \geq dist_{OD}$$

where $node_{s,h}$ denotes the node for the $s$-th stop in the $h$-th combination. If the condition is respected, the fuel amount to be refueled by one vehicle on each node for the $s$-th stop according to the refueling strategy $k$ of the path $p$ $\left(a^k_{node_s,p}\right)$ is determined as:

$$a^k_{node_s,p} = r_{node_s,h} \qquad if\ s \in [1, S_p - 1]$$

$$a^k_{node_s,p} = dist_{OD} - \sum_{s=1}^{S_p-1} r_{node_s,h} \qquad if\ s = S_p$$

In other words, for the first $S_p - 1$ stops the tank is filled up to its maximum, while for the last stop, the fuel amount is equal to the necessary residual quantity to reach destination with $VR_f = VR_i$.

By repeating this algorithm for all the paths in the dataset, the set of node combinations constituting the refueling strategies of each path $p$, $K_p$, and the set of the fuel amounts needed on each node $i$ of path $p$ according to each given refueling strategy $k$, $a^k_{i,p}$, are generated. These represent the input data for the optimization model. Depending on the refueling strategy, and the location of the first stop (in case of $S_p > 1$), a different fuel amount could be required on a same node. Further details of the algorithm are reported in supplementary material with a practical example.

### 2.4. Optimization model

The optimization model used in the framework is a re-formulation of the node-capacitated flow refueling location model (NC-FRLM) by Rose et al., adapted to a different input data structure obtained from the previous step.

The objective function (1) aims to minimize the number of stations to be placed in the network to satisfy the refueling demand of all the vehicles travelling across the network:

$$min \sum_{i \in N} x_i \tag{1}$$

subject to:

$$\sum_{k \in K^p} y^k_p = 1 \quad \forall p \in P \tag{2}$$

$$\sum_{p \in P} \sum_{k \in K^p} \left[ v_p \cdot a^k_{i,p} \cdot e_{vehicle} \cdot y^k_{i,p} \right] \leq c \cdot x_i \quad \forall\, i \in N \tag{3}$$

$$0 \leq y^k_p \leq 1 \quad \forall\, p \in P, k \in K^p \tag{4}$$

$$x_i \in \{0,1\} \quad \forall\, i \in N \tag{5}$$

$$y^k_{i,p} = y^k_p \quad \forall\, p \in P, k \in K^p, i \in k \tag{6}$$

| | |
|---|---|
| **Variables** | |
| $x_i$ | Binary variable. 1 if a station is placed in node i, 0 otherwise. |
| $y^k_p$ | Real positive variable. Fraction of vehicles on path $p$ refueling according to the refueling strategy $k$. |
| $y^k_{i,p}$ | Real positive variable. Fraction of vehicles on path $p$ refueling on node $i$ according to the refueling strategy $k$. |
| **Parameters** | |
| $v_p$ | Number of vehicles on the path $p$. |
| $a^k_{i,p}$ | Equivalent fuel amount, expressed in $km$, required by a vehicle of path $p$ on node $i$ according to the refueling strategy $k$. |
| $e_{vehicle}$ | Vehicle fuel consumption expressed in $kg_{H2}\cdot km^{-1}$. |
| $c$ | Node daily capacity: it is the maximum amount of fuel a node can supply daily, expressed in $kg$. |
| **Sets** | |
| $N$ | Set of all the $i$ nodes constituting the network. |
| $P$ | Set of all the $p$ paths across the network. |
| $K^p$ | Set of all the $k$ refueling strategies for the $p$-th path. |

Equation constraint (2) states that, for each path, the summation of the fractions of vehicles refueling according to any refueling strategy of that path must equal 1. In other words, each vehicle on the path must be refueled according to at least one refueling strategy.

Equation (6), introduced for formality, states that the fraction of vehicles of path $p$ refueling on each node $i$ constituting the refueling strategy $k$ according to that strategy is of course equal to the fraction of vehicles of path $p$ refueling according to strategy $k$. This equality is then used for equation (3): for each node, particularly those where a station is placed, the sum of the demand from vehicles on all the paths $p$ refueling at node $i$ according to all refueling strategies $k$ involving node $i$ must be less than or equal to the maximum overall node's daily capacity.

The framework was implemented in Pyomo [59] with CPLEX as the solver [60] with a MIPgap of $10^{-6}$. It was run with 3.48 GHz Apple M2 Pro Chip with 16 GB memory.

### 2.5. Case study

The Italian territory is chosen as case study to find the optimal sites for hydrogen refueling stations. Fig. 6 represents the Italian NUTS-2 regions, grouped by NUTS-1 region. For each region, the corresponding unique alphanumeric NUTS-2 code is provided, which will be used in Sections 3 and 4 to refer to the regions.

Together with the assumptions made in Section 2.1, other additional

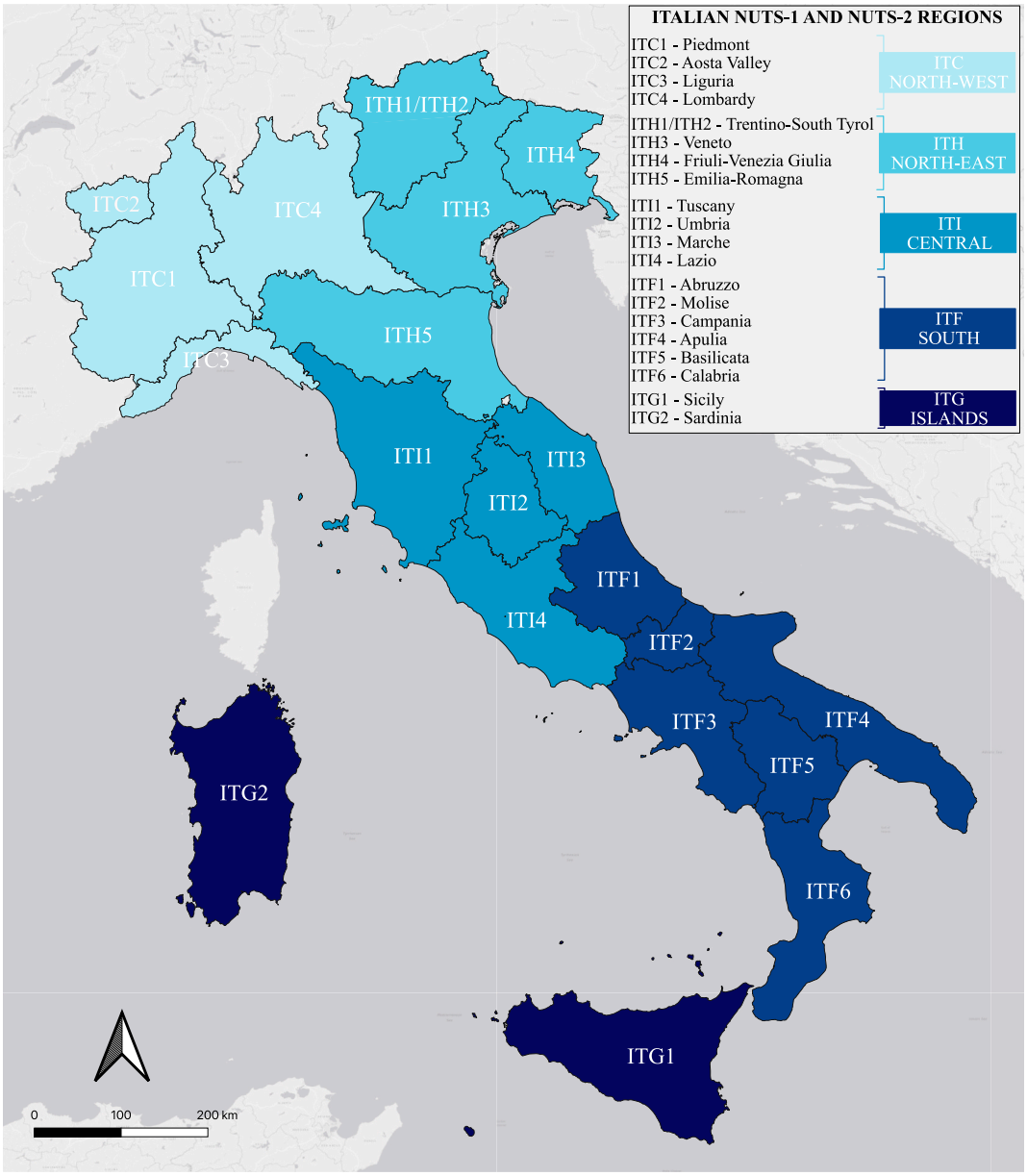


**Fig. 6.** Italian NUTS-2 regions grouped by NUTS-1 region.

hypotheses are made for the Italian case study.

- HRS capacity: HRS are capacitated based on the capacity constraints defined by H2 Mobility in Germany. These standard hubs have a daily capacity of 500 (small, S), 1000 (medium, M), 2000 (large, L) or 4000 kg (extra-large, XL) [61]. Since each node is assumed to capture the traffic flow in both directions, the actual node capacity is two times the HRS capacity. Thus, each node is assumed to host two stations (one for each direction), giving a maximum daily capacity of 8000 kg per node as upper bound for the constraint (3).
- FCHEV penetration: According to the Italian NRRP, a penetration of 5–7% is expected by 2030 for FCHEVs in the HD segment [16]. Therefore, in this work we investigate the design of an HRS network to satisfy the demand associated with a 10% FCHEV penetration. The traffic flow for each path $v_p$ is given by:

$$v_{p,FCHEV} = v_{p,2030} \bullet 0.1$$

where $v_{p,2030}$ is the expected traffic flow for the year 2030 on a certain path, and 0.1 a conservative over-estimation of the forecasted FCHEVs share. Only paths travelled by at least 10 vehicles per day are considered in the analysis.

- Vehicle range: considering the wide range of autonomy declared by different FCHEV manufactures (from 350 to 1000 km, with the latter being overly optimistic), a value of 600 km is chosen for the $VR_{max}$. This is a reasonable compromise between technological limitations and expected improvements in the short to mid-term, based on the technology review by Basma et al. [9].
- Path selection: since FCHEVs have similar or even better performances than other solutions (such as BEVs) in mid and long-distance transport operations, particularly in terms of Total Cost of Ownership (TCO) [11,12], only paths with a travelled distance of 100 km or more are considered. A total of 2202 paths are thus considered, with length ranging from 100 km to 1013 km and a median value of 243 km.
- Initial vehicle range: $VR_i$ is set equal to 300 km as this value minimizes the number of required HRS nodes for vehicles with $VR_{max}$ = 600 km, as presented in detail in Section 3.2.

- After the framework is executed, for each node where $x_i$ is equal to 1 (i.e., all the nodes in which an HRS is placed), the actual capacity of the refueling stations is determined. This is done by evaluating the fuel demand at the node and assigning the closest available capacity to match the demand. Once the capacity is assigned, the utilization factor ($UF_i$) is calculated as the ratio between the actual demand met at the node and its maximum theoretical daily capacity. This is expressed as:

$$UF_i = \frac{\sum_{p\in P}\sum_{k\in K^p} v_p \cdot a^k_{i,p} \cdot e_{vehicle} \cdot y^k_{i,p}}{c_i}$$

### 2.6. $CO_2$ emissions scenarios

The local production of hydrogen in each region required to satisfy the HD vehicles demand will have an associated amount of $CO_2$ emissions depending on the primary energy source used to produce the hydrogen. Therefore, we quantify three scenarios to be compared with the *as-is* scenario, assuming that the HD vehicles have an average emission factor of 783 $gCO_2 \cdot km^{-1}$ [62]. For the as-is scenario, the emissions are estimated for the whole road freight transport sector, including paths not considered for the transition to FCHEVs (i.e., paths with $dist_{OD} < 100$ km and travelled by less than 10 vehicles per day). For the current Italian energy mix, an emission factor of 297 $gCO_2 \cdot kWh^{-1}$ is considered [63].

- Scenario 1 (business-*as*-usual): in this scenario, hydrogen is produced through electrolysis powered by the current Italian energy mix, assuming it remains unchanged until 2030.
- Scenario 2 (Actual RES generation): in this scenario, the net difference between renewable electricity produced ($E_{ren,prod}$) and consumed ($E_{ren,cons}$) is evaluated for each Italian NUTS-2 region. This difference ($E_{ren,avbl}$), when positive, represents the surplus of renewable electricity generated in each region, which nowadays is exported to other regions. It is assumed that this net balance is used for the local production of hydrogen. For each region, it is assessed whether the current amount of surplus renewable electricity is sufficient to meet the regional yearly hydrogen production demand ($E_{H2,y}$), assuming a specific energy consumption of 55 $kWh \cdot kg^{-1}_{H_2}$ for the electrolysis [64]. If not, it is assumed that the surplus hydrogen would be produced using the current national energy mix.
- Scenario 3 (Additional PV power): in this scenario, in the regions where there is shortage of RES generation ($E_{ren,avbl}$ negative), the equivalent additional photovoltaic (PV) power to be installed ($P_{ren,add}$) in each region is evaluated to ensure that all the hydrogen production is green. This calculation consider the specific PV producibility equivalent hours ($H_{eq}$) for each region [65]. The analysis focuses on solar PV due to its more uniform availability across the country with respect to other renewable sources (e.g., wind) [66]. Furthermore, incorporating other renewable sources into the analysis would require detailed assumptions about the regional energy mix, which was beyond the scope of this study. Finally, since other sources typically exhibit higher capacity factors, we adopted a conservative approach to estimate the additional renewable capacity to be installed.

## 3. Results

### 3.1. Optimal HRS location

This section presents the results of our work, which aims to minimize the number of stations needed to satisfy the refueling demand of all vehicles travelling across the network. The simulation framework described in the previous sections was applied to find the optimal configuration for the HRS network on the TEN-T Italian network and it took 7.76 s to solve. Further details about framework performances are available in Section III of the supplementary material.

The optimal location for HRS needed to satisfy a 10% share of FCHEV in Italy is represented in Fig. 7. A total of 78 nodes have been identified: 29 of size S, 14 of size M, 23 of size L and 12 of size XL.

Even though the stations are almost equally spread across the Italian territory in terms of number of HRS per NUTS-1 region, a clear geographical trend is evident in terms of nodes size and overall hydrogen demand fraction, as showed in Fig. 8.

- South Italy (ITF1: Abruzzo, ITF2: Molise, ITF3: Campania, ITF4: Apulia, ITF5: Basilicata, ITF6: Calabria) primarily features small-sized stations, with only 6 out of 18 being size M (3) and L (3).
- The islands (ITG1: Sicily, ITG2: Sardinia) have 10 HRS nodes, mainly size S (8), with an average UF of 54%.
- Central Italy (ITI1: Tuscany, ITI2: Umbria, ITI3: Marche, ITI4: Lazio) shows a more homogeneous distribution of HRS size with an average size higher than the southern regions and with an average UF of 63%.
- North-East Italy (ITH1/ITH2: Trentino-South Tyrol, ITH3: Veneto, ITH4: Friuli-Venezia Giulia, ITH5: Emilia-Romagna) has 16 stations, 6 of which are size L and 7 size XL. This area accounts for the 39% of the whole daily hydrogen demand and has the highest average UF at 83.5%.
- North-West Italy (ITC1: Piedmont, ITC2: Aosta Valley, ITC3: Liguria, ITC4: Lombardy)), accounts for 27.8% of the total daily hydrogen demand, with 16 stations mainly of size L (6) and XL (4). Only one station is S-sized, located near the city of Turin, with an UF of 73.2%.

Notably, no station is placed in Molise, Aosta Valley, Trentino-South Tyrol and Friuli-Venezia Giulia (ITF2, ITC2, ITH1/ITH2 and ITH4, respectively). In the latter three regions, this is due to the case study focusing only on national road freight transport. Given that 4 out of 7 road links to other European countries are in these regions, it is reasonable to expect some HRS to be placed there if the international (i.e., cross-border) transport is also considered.

The median utilization factor is 67.5%. Among the 78 HRS nodes, 14 have $UF_i < 50\%$ and they all have a capacity of 1000 kg and they are almost all located (10 out of 14) in the South or in the Islands. As the node capacity increases, the UF tends to vary in a shorter range and its median value tends to increase. Size S HRS nodes have $UF_i$ ranging from 6 to 99%, with a median value of 49%, while size XL HRS nodes have $UF_i$ ranging from 53 to 100%, with a median value of 86% (Fig. 9).

Overall, about 182815 kg of hydrogen per day are needed all around the network considering $e_{vehicle}$ of 0.075 $kg_{H_2} \cdot km^{-1}$, which is equal to approximately 47531 $t_{H_2}$ per year and 2.61 *TWh* of renewable electricity, in case of exclusive use of green hydrogen, assuming a specific energy consumption of 55 $kWh \cdot kg^{-1}_{H_2}$ for the electrolysis. This result is in line with the expected hydrogen demand for transportation in Italy from other institutional sources [67].

### 3.2. $CO_2$ emissions and green hydrogen production

To effectively reduce emissions in the transport sector, the hydrogen used by the trucks must be green, i.e., produced exclusively from renewable energy sources. This would ensure that the emissions associated with the operation of FCHEVs are zero. Therefore, different scenarios, presented in Section 2.6, have been compared in terms of required expansion of the renewable capacity in each region (Fig. 10) and emission reduction of the road freight transport system (Fig. 11).

The available renewable electricity $E_{ren,avbl}$ (i.e., the overproduction that is currently exported to other regions) is already sufficient to meet the yearly demand for green hydrogen production within the region in 10 out of 17 NUTS-2 regions with at least one HRS. This is particularly evident in the southern regions and in the islands, which have lower hydrogen demand, and in regions with high renewable production (e.g.,

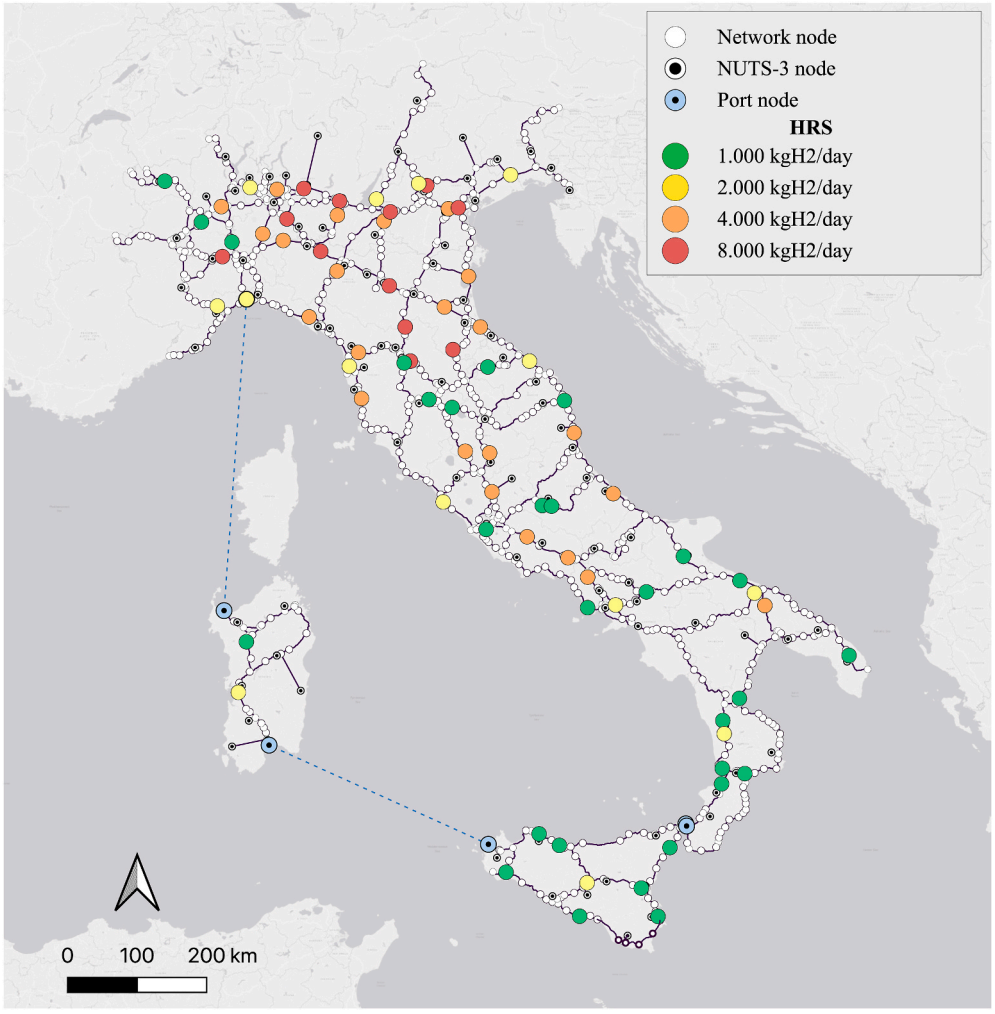


**Fig. 7.** Solution of the NC-FRLM for a FCHEV share of 10%, VRi equal to 300 km and VRmax equal to 600 km.

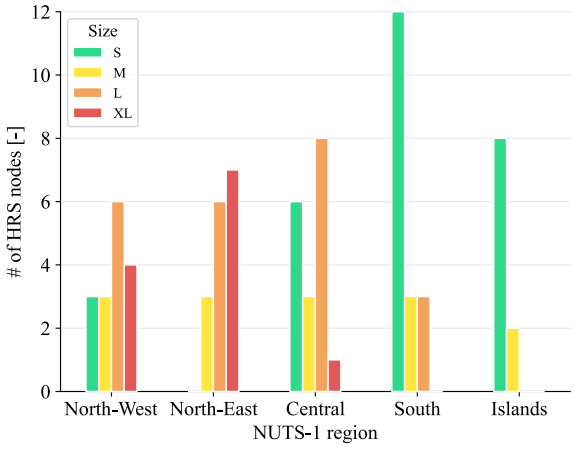


**Fig. 8.** HRS distribution by size and by NUTS-1 region.

ITC4 and ITI1, respectively first and third region in Italy for renewable electricity production). On the other hand, in the remaining 7 NUTS-2 regions, $E_{ren,avbl}$ is not sufficient yet. Notably, Emilia-Romagna (ITH5) and Veneto (ITH3), two of the regions with the highest hydrogen demand (23.6 and 15.8% of the total, respectively), show a significant mismatch in terms of renewable capacity needed. On the other hand, in Liguria (ITC3), which has the seventh highest value of $E_{H2,y}$ (93 *GWh*), only the 7.5% of the demand can be met with the current RES generation.

The $CO_2$ emissions of the national road freight transport sector without considering intra-regional trips in the *as-is* scenario amounts to around 7.2 $Mton_{CO_2}$, as depicted in Fig. 11. In Scenario 1 the emissions would even increase up to the 4% with respect to the *as-is* scenario, highlighting the necessity to increase the renewable energy share in the energy mix. In Scenario 2, as only a portion of the total energy required for the electrolysis (≈ 27%) is taken from the grid, an emission reduction of about 3.6% is expected. Finally, in Scenario 3, as the whole production is covered by renewable electricity, requiring the installation of 368 *MW* additional PV capacity, emissions are reduced by the 6.5%. This because, even though the FCHEVs share is considered to be 10% for this case study, the transport segment investigated (i.e., paths with $dist_{OD} >$ 100 km and travelled by at least 10 vehicles per day) accounts for about the 65% of the whole freight transport system in terms of vehicle-kilometers. It is worth underling that the "ICE trucks" bars shown in Fig. 11 represent also the emissions associated to the vehicles travelling on the routes not considered for the transition to FCHEVs.

### 3.3. Sensitivity analysis on vehicle ranges

The impact of some parameters – namely initial vehicle range, $VR_i$, and maximum achievable vehicle range, $VR_{max}$ – on the solution has

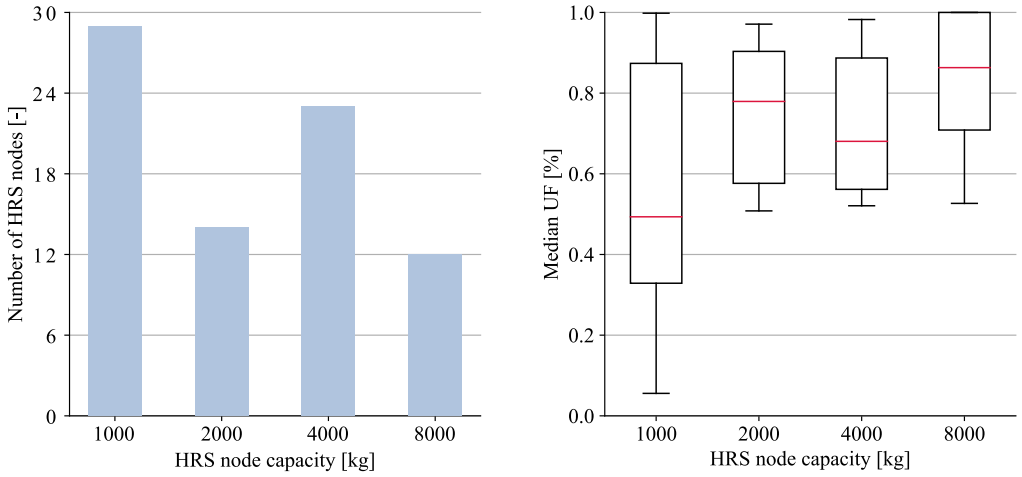


**Fig. 9.** – (a) HRS nodes distribution and (b) median utilization factor by size.

been evaluated. As shown in Section 2.3, $VR_i$ plays a crucial role in determining the potential refueling strategies on each path, and thus influences the final solution of the problem. On the other hand, the effect of $VR_{max}$ is less significant. This is because the normative constraint on the maximum distance between each stop ($dist_{max}$) affects only few cases. In fact, only the 4% of the total vehicle-kilometers are associated to paths with a $dist_{OD}$ higher than 720 km.

$VR_{max}$ was varied in a range from 400 to 800 km. Since the scope of the work is to design a HRS infrastructure for the main road network, the NUTS-3 nodes are not considered as candidate sites for the hubs. Therefore, $VR_i$ was varied from 150 km to $VR_{max}$ – 150 km. Setting values below this range can lead to infeasibility in the problem solution with the chosen network topology. Since the nodes are not equally spaced, there may not be HRS candidate sites within 150 km of the starting point. It is important to note that this lower bound is specific to the network topology used in the case study and may be different for other networks. Also, it could be easily overcome by adding other candidate site nodes in the starting part of each path, but this was out of the scope of our work.

Fig. 12 shows how the number of HRS nodes varies by varying $VR_i$ and $VR_{max}$. When $VR_i$ is low, the first stop occurs within a short distance, resulting in a high number of hubs placed closer to the path origin points. As $VR_i$ increases, it becomes more likely to intercept the path of other O-D pairs, creating opportunities to place a HRS where it can serve multiple O-D paths. This leads to a decrease in the number of HRS needed.

However, if $VR_i$ increases over a certain threshold, the number of HRS increases again. Since, $VR_f$ is assumed to be equal to $VR_i$, the last refuel stop must occur not farther than $VR_{max} - VR_i$ from the destination. As $VR_i$ (and thus $VR_f$) increases, hubs will be placed closer to the destination node. We found that the minimum number of HRS nodes for each value of $VR_{max}$ occurs when $VR_i$ is approximately half of $VR_{max}$. This value balances the maximization of the shared routes segments (which occurs at high $VR_i$ values) and of the availability of free space in the tank (which occurs at lower $VR_i$ values). As the $VR_{max}$ is increased, lower values of $VR_i$ result in higher fuel tank availability, reducing the number of refueling occasions needed and thus the overall number of HRS nodes. Additionally, the curve tends to flatten for the "central" values of $VR_i$, making the solution less dependent on $VR_i$, in terms of number of HRS nodes. A detailed example of this behavior is presented in the supplementary material. Furthermore, an extensive analysis on the impact of $VR_i$ and $VR_{max}$ on an ideal network with equally spaced nodes and with paths having the same length is provided, showing that any deviation from the ideal behavior (i.e., number of stations decreasing by increasing $VR_{max}$ and $VR_i$ until a certain threshold) is due to the specific network topology and to the paths' characteristics.

Our results show that most solutions have a number of stations ranging from 75 to 88, meaning that in average 80 hubs are needed to satisfy the demand of a 10% of share of FCHEVs in the HD road freight transport sector, depending on the chosen technological parameters.

## 4. Discussion

In this work, we investigated the optimal placement and sizing of hydrogen refueling stations (HRS) required to support a 10% share of fuel cell heavy-duty electric vehicles (FCHEVs) in the Italian road freight transport sector. The approach utilized the optimization node-capacitated flow refueling location model (NC-FRLM) to determine the number and location of HRS needed to meet the hydrogen demand. Our results show that an average of 80 hubs are required, with the number of stations ranging from 75 to 88, depending on the chosen technological parameters. It is worth mentioning that the seconds step of the framework, the data pre-processing (Section 2.3) aims to define the refueling strategies that allow completing the route with the fewest possible stops. While this assumption may potentially lead to a suboptimal global solution (e.g., requiring the opening of an additional refueling station on certain routes), it ensures that vehicles are not forced to make more stops in a close proximity. This is particularly important in the context of freight transport, where operational efficiency is a key concern. Overall, around 183 t of hydrogen per day are needed across the network, which is equal to approximately 2.61 TWh of renewable electricity per year, in case of exclusive use of green hydrogen. The distribution of hydrogen demand across Italy reveals significant regional differences. In the southern regions and islands, the hydrogen demand is lower and smaller stations are primarily placed. In contrast, the central and northern regions, particularly Lombardy (ITC4) Emilia-Romagna (ITH5) and Veneto (ITH3) have a higher concentration of larger stations. The analysis indicates that the total additional renewable energy sources (RES) capacity needed to achieve 100% green hydrogen production, as per Scenario 3, requires the installation of 368 MW of new photovoltaic (PV) power. This regional breakdown highlights the varying capabilities and needs across different parts of the country, emphasizing the importance of localized solutions for effective hydrogen infrastructure development.

To the best of the authors' knowledge, no other study has specifically targeted the Italian national road freight transport system for an optimal siting and dimensioning of the HRS infrastructure. Guzzini et al. [68] proposed a GIS-based tool to locate and design power-to-gas and power-to-hydrogen plants in Italy minimizing the levelized cost of hydrogen. However, their approach did not differentiate between light-duty and heavy-duty vehicle fuel requirements, focusing instead on

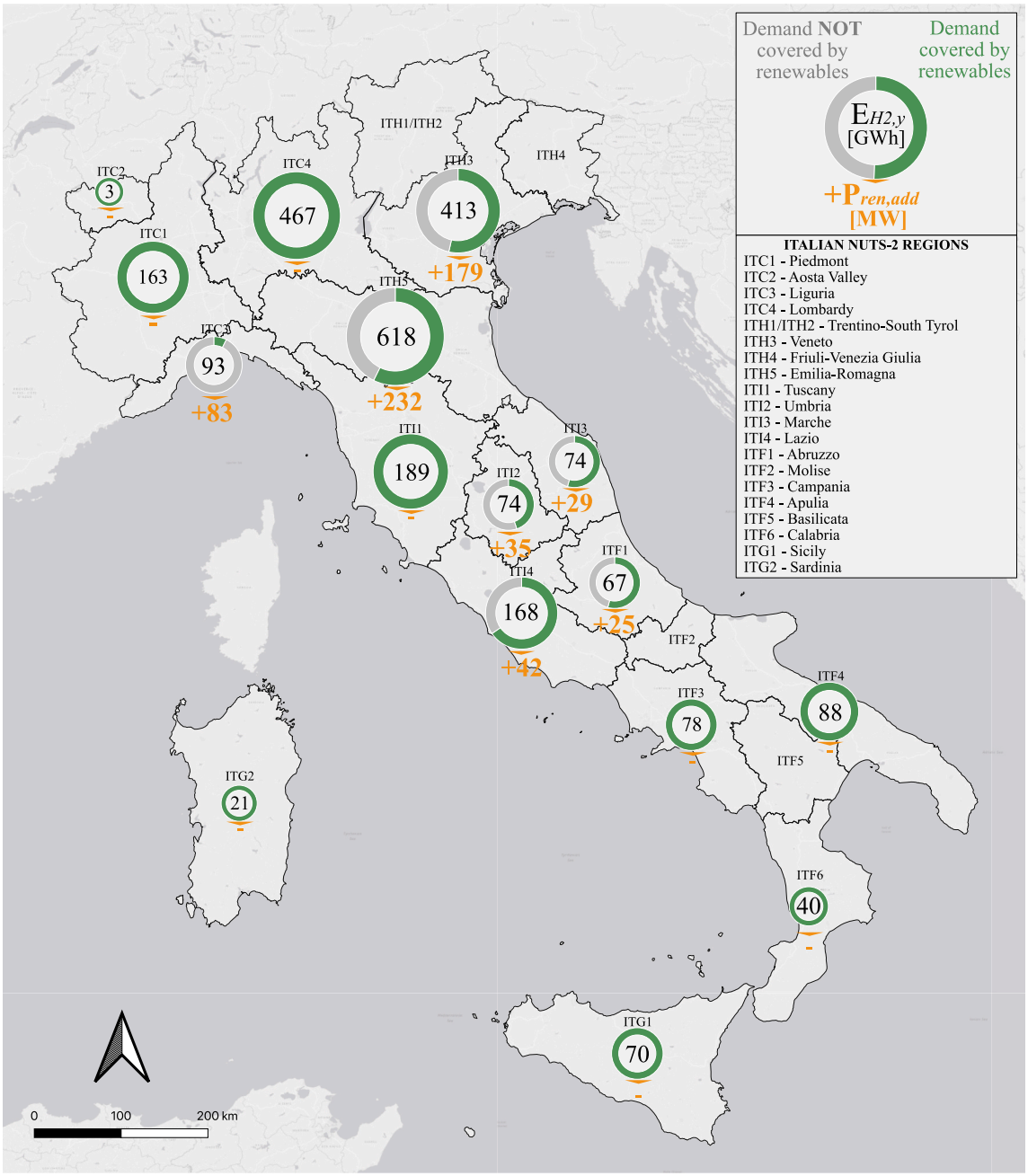


**Fig. 10.** Electricity demand for electrolysis and new renewable capacity needed to have 100% green hydrogen per NUTS-2 region. (For interpretation of the references to colour in this figure legend, the reader is referred to the Web version of this article.)

re-converting all the existing highway refueling stations to HRS. Our study provides a more focused analysis on the specific needs of the HD road freight transport sector, which is reflected in the differences in HRS distribution and sizing. While both studies agree that larger stations are expected to be concentrated in the north and central-north regions, particularly in ITC4, ITH5 and ITI1, our work offers a detailed assessment of the infrastructure required to support a 10% FCHEV penetration, highlighting the necessity of additional RES capacity to ensure green hydrogen production.

Finally, it is worth comparing our findings with the distribution of 54 road HRS financed under the Investment 3.3 of the Italian NRRP or proposed by stakeholders [69]. As a premise, it has to be mentioned that unfortunately the comparison can be limited to very few aspects, as many key specifications of the refueling stations defined in the plan are missing or not publicly available. First of all, our study explicitly targets the decarbonization of HD freight transport, while it is not clear if the announced development plan includes a wider spectrum of transport sectors (e.g., public or private transportation). Nonetheless, our study reveals a more heterogeneous distribution of hubs per geographical area. In particular, in the NRRP plan only 20 hubs out of 54 are located south of ITH5, with all other located in the northern Italy. This distribution suggests a less uniform adoption of FCHEVs across the country compared to our model.

While the exact position and the daily capacity of the financed hubs is unknown, we compared the number of hubs per NUTS-2 region with respect to our model results (Fig. 13). In the northern regions, the financed stations outnumber those in our model (31 against 24). This is particularly evident in the border regions Aosta Valley, Trentino South-Tyrol and Friuli-Venezia Giulia (ITC2, ITH1/ITH2 and ITH4, respectively), where 9 stations have been financed or proposed, compared to

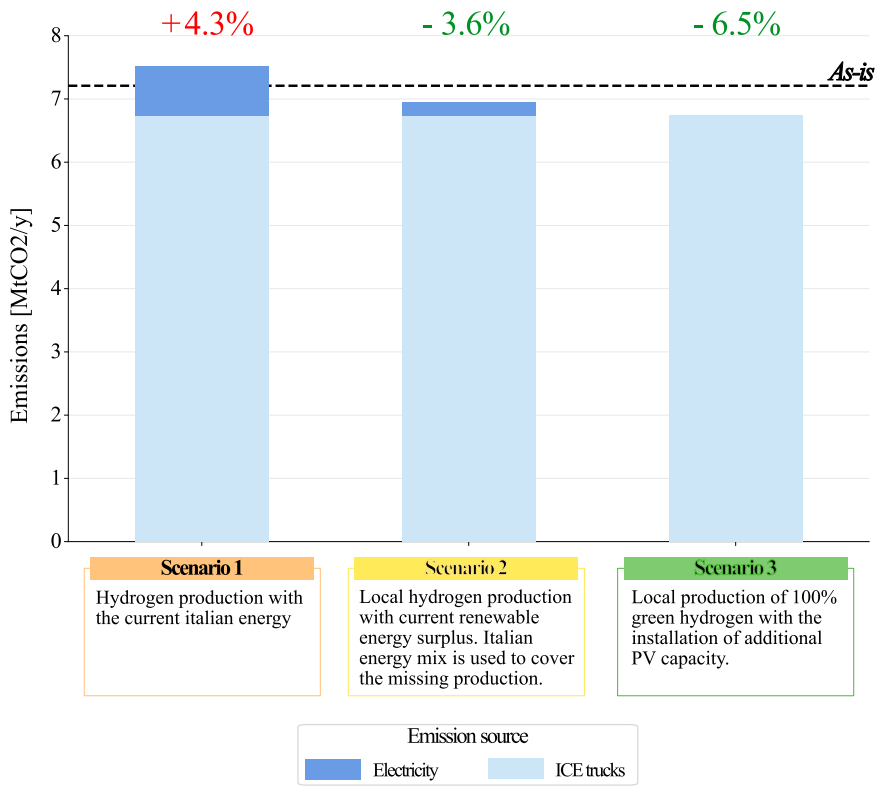


**Fig. 11.** Emissions by source in each scenario.

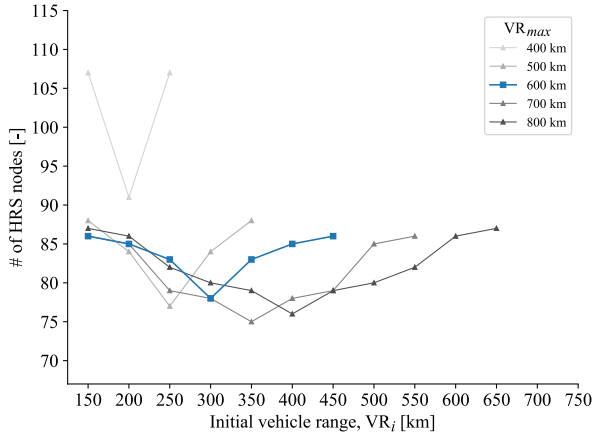


**Fig. 12.** – Number of HRS nodes as a function of the initial vehicle range for different values of maximum vehicle range.

the 1 placed by our model (in ITC2). This aligns with the NRRP goal of decarbonizing specific international routes, such as the Green and Digital and the Western-Eastern corridors. This can be seen as a limitation of our model as it does not consider cross-border international transport. On the other hand, the NRRP infrastructure significantly underdimensions the number of refueling stations in other regions, particularly Emilia-Romagna (ITH5) and Tuscany (ITI1). These regions are critical transit points for medium to long-distance routes between northern to southern Italy, and only 5 hubs seem a noticeable underestimation of the hydrogen demand across these routes. Sicily (ITG1), with its 9 NUTS-3 nodes, is the most under-dimensioned region by NRRP plan with respect to our model. This may be due to our model assumption that refueling is available for all the vehicles travelling from any origin to any destination. Sicily in fact has multiple access points to the road network, resulting in different starting or ending segments for routes beginning or ending there.

Our model, despite being a useful evaluation tool for preliminary considerations for the design of an optimal developed HRS infrastructure, has some intrinsic limitations which should be clarified.

As it has been shown in Section 3.3, the results may be affected significantly by some parameters, such as the assumed initial vehicle range $VR_i$ and by the maximum vehicle range $VR_{max}$. Since it is hard to find publicly available data about drivers' behavior and refueling habits, it is important to make plausible assumptions. Too conservative or too optimistic ones, in fact, may lead to over-size or under-size the infrastructure. Also considering that all the vehicles start with the same $VR_i$ and arrive with the same $VR_f = VR_i$ may be unrealistic, since with this approach a refueling stop is performed also when $dist_p < VR_i$. On the other hand, this assumption is useful to represents the actual energy requirement for all the routes.

Vehicles are assumed to have all the same technical specifications, especially in terms of maximum achievable vehicle range. This is a strong assumption since the declared autonomy by the different constructors nowadays varies in a range from 350 to 1000 km [9]. Also considering the fuel consumption as only depending on the travelled distance leads to overestimate the actual $VR_{max}$, since other factors may have an impact on it too, as it was highlighted in Section 2.1.

The model has constraints only on the daily amount of fuel that a station can supply. In fact, since the traffic flow is assumed to be constant and it is only characterized by a daily value, limitations on a more refined temporal scale (e.g., hourly) are not delineated. This may lead to higher waiting times for the drivers for example if all the dispensers are being used in a certain moment. Furthermore, it is assumed that each node has two stations of equal size, one for each direction. While the overall nodal capacity (i.e., 8000 kg per day) is respected, in practice, it is possible that the maximum daily capacity for one direction (i.e., 4000

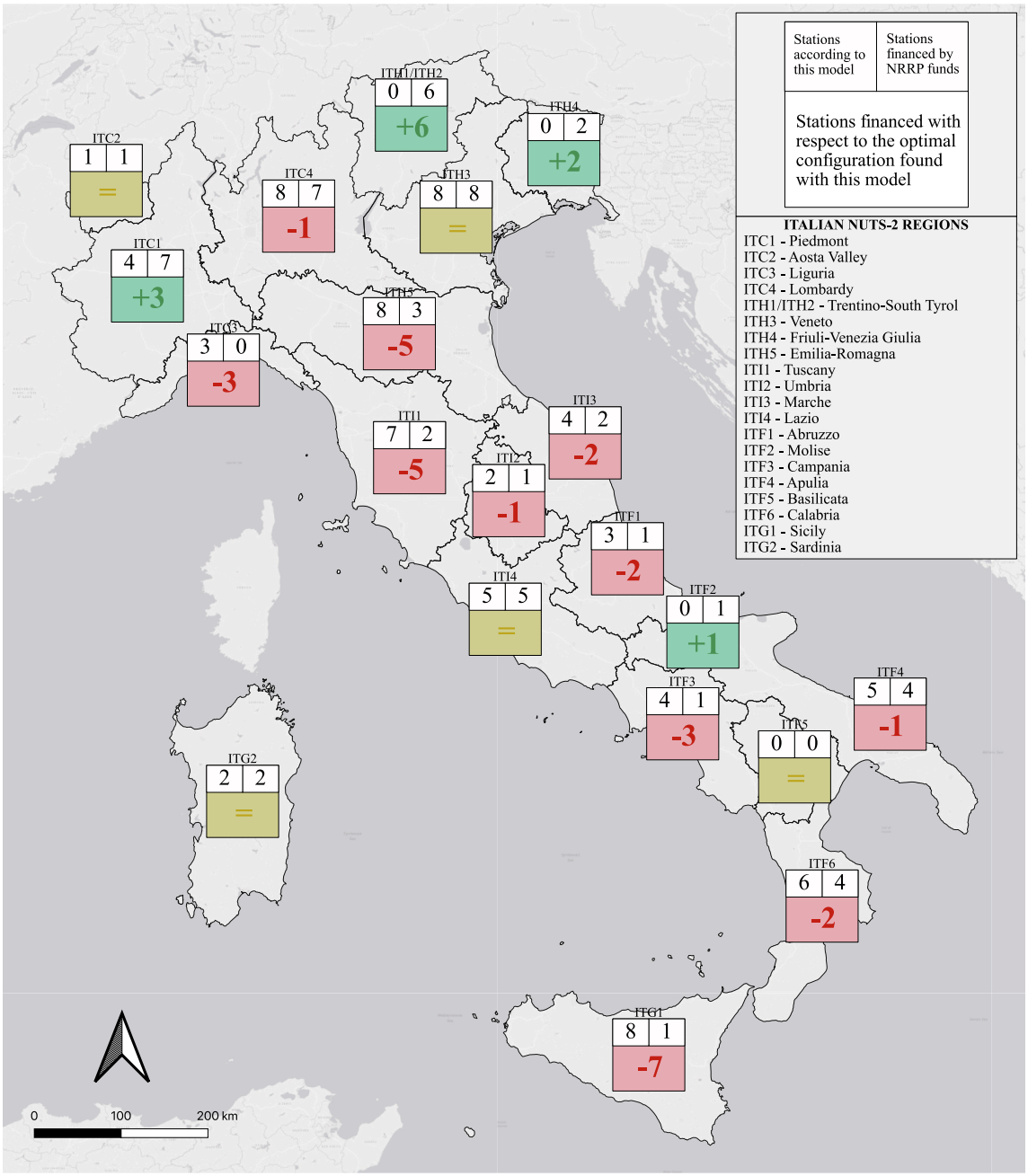


**Fig. 13.** Comparison of the number of stations placed by our framework and those financed by NRRP funds per NUTS-2 region.

kg per day) could be exceeded.

An important approximation is also to assume all the paths starting (or ending) from the same node within an origin NUTS-3 region. The actual travelled distance may be significantly different, as secondary or rural roads are not included in the network. This may lead to over- or under-estimate the actual distance travelled before entering or after exiting the main road network.

## 5. Conclusions

In this work we proposed a GIS-based framework for the optimal location of hydrogen refueling stations (HRS), integrating normative driving time constraints with other technical limitations. The proposed framework can be a useful evaluation tool to strategically site HRS, both for stakeholders and policymakers, and therefore to support decarbonization initiatives [70]. We applied this framework to a case study of the Italian high-speed road network. The approach employed the node-capacitated flow refueling location model (NC-FRLM) to optimize the number and locations of HRS required to meet hydrogen demand. The energy demand was derived from the ETISPlus for transported goods and adapted by considering only national road freight transport within Italian NUTS-3 regions.

It was found that at least 76 HRS nodes are required all around the network, for a 10 % share of hydrogen vehicles of the total circulating vehicles by 2030. Overall, about 183 t of hydrogen per day are needed all around the network, which is equal to approximately 47500 $t_{H_2}$ per year and 2.61 *TWh* of renewable electricity, in case of exclusive use of green hydrogen. Hence, an equivalent additional capacity of 368 MW of PV plants is required in order to allow green hydrogen production locally in each NUTS-2 region with renewable electricity, allowing to reduce the emissions of the road freight transport up to the 6.5%. Finally, it was highlighted that the NRRP infrastructure is significantly

under-dimensioned in critical regions, such as Emilia-Romagna (ITH5), Tuscany (ITI1) and Sicily (ITG1).

We find valuable to outline the following recommendations for future works.

- A stochastic approach on the initial vehicle range parameter would allow a more realistic representation of the actual fuel demand on each station, as it was shown that this parameter may have a significant impact on the required number of HRS on the network.
- A more realistic representation of the actual fuel consumption rate would also contribute to a better representation of the actual fuel demand, taking into account the impact of other factors, such as road slope, external temperature and so on, based on georeferenced and registry data.
- Cross-border international transport should be included too, performing a more comprehensive analysis (e.g., at European scale), as it seems realistic that the adoption of FCHEVs and the deployment of the refueling infrastructure will happen primarily on specific international corridors.
- A more refined temporal analysis demand side (e.g., on hourly basis) would allow to better characterize the station utilization behavior and to determine the actual interaction of the HRS network with the energy system (especially, the electric grid infrastructure).

## CRediT authorship contribution statement

**Antonio De Padova:** Writing – original draft, Visualization, Software, Methodology, Investigation, Formal analysis, Data curation. **Daniele Salvatore Schiera:** Writing – review & editing, Visualization, Software, Methodology, Data curation. **Francesco Demetrio Minuto:** Writing – review & editing, Visualization, Supervision, Methodology, Conceptualization. **Andrea Lanzini:** Writing – review & editing, Supervision, Funding acquisition, Conceptualization.

## Declaration of competing interest

The authors declare that they have no known competing financial interests or personal relationships that could have appeared to influence the work reported in this paper.

## Acknowledgements

The authors would like to express their deepest gratitude to Alessandro Agostini, Claudio Carbone and Francesco Gracceva from ENEA for the insightful feedback and constructive discussion that enhanced the quality of this research.

A. De Padova carried out this study within the PhD programme funded by ENEA as part of the project H206, Program agreement between MiTE and ENEA for the regulation of relations concerning the conduct of research activities within the framework of the NRRP - Mission 2 - Component 2 - Investmend 3.5, funded by the European Union under the Next Generation EU initiative, Operational Research Plan "Research and development of thechnologies for the hydrogen supply chain".

F.D. Minuto carried out this study within Ministerial Decree no. 1062/2021 and received funding from the FSE REACT-EU - PON Ricerca e Innovazione, 2014 - 2020.

## Appendix A. Supplementary data

Supplementary data to this article can be found online at https://doi.org/10.1016/j.ijhydene.2024.11.086.

## References

[1] European Commission. Directorate general for communication, 'European green deal - delivering on our targets. Publications Office of the European Union; 2021 [Online]. Available: https://data.europa.eu/doi/10.2775/352471.
[2] European Environment Agency. Decarbonising road transport: the role of vehicles, fuels and transport demand. LU. Publications Office; 2022 [Online]. Available: https://data.europa.eu/doi/10.2800/68902. [Accessed 24 April 2024].
[3] European Automobile Manufacturers' Association (ACEA). Vehicles on European roads - 2024. 2024.
[4] European Automobile Manufacturers' Association (ACEA). Factsheet - CO2 standards for heavy duty vehicles [Online]. Available: https://www.acea.auto/files/Fact-sheet-CO2_standards_for_heavy_duty_vehicles.pdf. [Accessed 11 June 2024].
[5] European Environment Agency. Reducing greenhouse gas emissions from heavy-duty vehicles in Europe. 2022.
[6] Cunanan C, Tran M-K, Lee Y, Kwok S, Leung V, Fowler M. A review of heavy-duty vehicle powertrain technologies: diesel engine vehicles, battery electric vehicles, and hydrogen fuel cell electric vehicles. Clean Technol Jun. 2021;3(2). https://doi.org/10.3390/cleantechnol3020028. Art. no. 2.
[7] H. Basma, 'Battery electric tractor-trailers in the European Union: a vehicle technology analysis'.
[8] Pramuanjaroenkij A, Kakaç S. The fuel cell electric vehicles: the highlight review. Int J Hydrogen Energy Mar. 2023;48(25):9401–25. https://doi.org/10.1016/j.ijhydene.2022.11.103.
[9] Basma H, Rodríguez F. Fuel cell electric tractor-trailers: technology overview and fuel economy. 2022.
[10] European Parliament. Regulation (EC) No 561/2006 of the European Parliament and of the Council of 15 March 2006 on the harmonisation of certain social legislation relating to road transport and amending Council Regulations (EEC) No 3821/85 and (EC) No 2135/98 and repealing Council Regulation (EEC) No 3820/85 (Text with EEA relevance) - declaration, vol. 102; 2006 [Online]. Available: http://data.europa.eu/eli/reg/2006/561/oj/eng. [Accessed 13 June 2024].
[11] Guandalini G, Campanari S. Well-to-wheel driving cycle simulations for freight transportation: battery and hydrogen fuel cell electric vehicles. In: 2018 international conference of electrical and electronic technologies for automotive. Milan: IEEE; Jul. 2018. p. 1–6. https://doi.org/10.23919/EETA.2018.8493216.
[12] Ruf Yvonne, Baum Markus, Zorn Thomas, Menzel Alexandra, Rehberger Johannes. Fuel Cells Hydrogen Trucks: heavy Duty's high performance green solution. Study report. 2020.
[13] Anselma PG, Belingardi G. Fuel cell electrified propulsion systems for long-haul heavy-duty trucks: present and future cost-oriented sizing. Appl Energy Sep. 2022;321:119354. https://doi.org/10.1016/j.apenergy.2022.119354.
[14] Clean Hydrogen Partnership. Hydrogen refuelling stations | European hydrogen observatory [Online]. Available: https://observatory.clean-hydrogen.europa.eu/hydrogen-landscape/distribution-and-storage/hydrogen-refuelling-stations. [Accessed 13 June 2024].
[15] Genovese M, Fragiacomo P. Hydrogen refueling station: overview of the technological status and research enhancement. J Energy Storage May 2023;61:106758. https://doi.org/10.1016/j.est.2023.106758.
[16] Italia Domani. National Recovery and resilience plan (NRRP) #NextGenerationItalia [Online]. Available: https://www.governo.it/sites/governo.it/files/PNRR.pdf; 2021.
[17] IEA. The Future of Hydrogen: seizing today's opportunities. Report for the G20, Japan. Jun. 2019.
[18] Isaac N, Saha AK. A review of the optimization strategies and methods used to locate hydrogen fuel refueling stations. Energies Jan. 2023;16(5). https://doi.org/10.3390/en16052171. Art. no. 5.
[19] Lin R-H, Ye Z-Z, Wu B-D. A review of hydrogen station location models. Int J Hydrogen Energy Aug. 2020;45(39):20176–83. https://doi.org/10.1016/j.ijhydene.2019.12.035.
[20] Balas E, Padberg MW. On the set-covering problem. Oper Res 1972;20(6):1152–61.
[21] Kang JE, Recker W. Strategic hydrogen refueling station locations with scheduling and routing considerations of individual vehicles. Transp. Sci. Nov. 2015;49(4):767–83. https://doi.org/10.1287/trsc.2014.0519.
[22] Church R, Velle CR. The maximal covering location problem. Pap Reg Sci Jan. 1974;32(1):101–18. https://doi.org/10.1111/j.1435-5597.1974.tb00902.x.
[23] Frade I, Ribeiro A, Gonçalves G, Antunes AP. Optimal location of charging stations for electric vehicles in a neighborhood in Lisbon, Portugal. Transp. Res. Rec. J. Transp. Res. Board Jan. 2011;2252(1):91–8. https://doi.org/10.3141/2252-12.
[24] Gündüz SB, Geçici E, Güler MG. Locating hydrogen fuel stations: a comparative study for Istanbul. Int J Hydrogen Energy Jan. 2024;52:1234–46. https://doi.org/10.1016/j.ijhydene.2023.10.295.
[25] Hakimi SL. Optimum locations of switching centers and the absolute centers and medians of a graph. Oper Res Jun. 1964;12(3):450–9. https://doi.org/10.1287/opre.12.3.450.
[26] Nicholas MA, Handy SL, Sperling D. Using geographic information systems to evaluate siting and networks of hydrogen stations. Transp. Res. Rec. Jan. 2004;1880(1):126–34. https://doi.org/10.3141/1880-15.
[27] Kim H, Eom M, Kim B-I. Development of strategic hydrogen refueling station deployment plan for Korea. Int J Hydrogen Energy Jul. 2020;45(38):19900–11. https://doi.org/10.1016/j.ijhydene.2020.04.246.
[28] Minieka E. The m-Center Problem. SIAM Rev Jan. 1970;12(1):138–9. https://doi.org/10.1137/1012016.
[29] Hodgson MJ. A flow-capturing location-allocation model. Geogr Anal Jul. 1990;22(3):270–9. https://doi.org/10.1111/j.1538-4632.1990.tb00210.x.

[30] John Hodgson M, Rosing KE, Leontien A, Storrier G. Applying the flow-capturing location-allocation model to an authentic network: edmonton, Canada. Eur J Oper Res May 1996;90(3):427–43. https://doi.org/10.1016/0377-2217(95)00034-8.
[31] Shukla A, Pekny J, Venkatasubramanian V. An optimization framework for cost effective design of refueling station infrastructure for alternative fuel vehicles. Comput Chem Eng Aug. 2011;35(8):1431–8. https://doi.org/10.1016/j.compchemeng.2011.03.018.
[32] Li Y, Cui F, Li L. An integrated optimization model for the location of hydrogen refueling stations. Int J Hydrogen Energy Oct. 2018;43(42):19636–49. https://doi.org/10.1016/j.ijhydene.2018.08.215.
[33] Honma Y, Kuby M. Node-based vs. path-based location models for urban hydrogen refueling stations: comparing convenience and coverage abilities. Int J Hydrogen Energy Jun. 2019;44(29):15246–61. https://doi.org/10.1016/j.ijhydene.2019.03.262.
[34] Kuby M, Lim S. The flow-refueling location problem for alternative-fuel vehicles. Socioecon. Plann. Sci. Jun. 2005;39(2):125–45. https://doi.org/10.1016/j.seps.2004.03.001.
[35] Kuby M, Lim S. Location of alternative-fuel stations using the flow-refueling location model and dispersion of candidate sites on arcs. Netw. Spat. Econ. Jun. 2007;7(2):129–52. https://doi.org/10.1007/s11067-006-9003-6.
[36] MirHassani SA, Ebrazi R. A flexible reformulation of the refueling station location problem. Transp. Sci. Nov. 2013;47(4):617–28. https://doi.org/10.1287/trsc.1120.0430.
[37] Kim J-G, Kuby M. The deviation-flow refueling location model for optimizing a network of refueling stations. Int J Hydrogen Energy Mar. 2012;37(6):5406–20. https://doi.org/10.1016/j.ijhydene.2011.08.108.
[38] Jochem P, Brendel C, Reuter-Oppermann M, Fichtner W, Nickel S. Optimizing the allocation of fast charging infrastructure along the German autobahn. J Bus Econ Jul. 2016;86(5):513–35. https://doi.org/10.1007/s11573-015-0781-5.
[39] Upchurch C, Kuby M, Lim S. A model for location of capacitated alternative-fuel stations. Geogr Anal 2009;41(1):85–106. https://doi.org/10.1111/j.1538-4632.2009.00744.x.
[40] Stanëk R, Greistorfer P, Kastner AE. Advanced optimization models for the location of charging stations in e-mobility. Cent Eur J Oper Res Dec. 2023. https://doi.org/10.1007/s10100-023-00878-w.
[41] Rose PK, Nugroho R, Gnann T, Plötz P, Wietschel M, Reuter-Oppermann M. Optimal development of alternative fuel station networks considering node capacity restrictions. Transp. Res. Part Transp Environ Jan. 2020;78:102189. https://doi.org/10.1016/j.trd.2019.11.018.
[42] Rose PK, Neumann F. Hydrogen refueling station networks for heavy-duty vehicles in future power systems. Transp. Res. Part Transp Environ Jun. 2020;83:102358. https://doi.org/10.1016/j.trd.2020.102358.
[43] Nugroho R, Rose PK, Gnann T, Wei M. Cost of a potential hydrogen-refueling network for heavy-duty vehicles with long-haul application in Germany 2050. Int J Hydrogen Energy Oct. 2021;46(71):35459–78. https://doi.org/10.1016/j.ijhydene.2021.08.088.
[44] European Commission. Statistical office of the European union. Statistical regions in the European Union and partner countries: NUTS and statistical regions 2021. 2022 edition. LU: Publications Office; 2022 [Online]. Available: https://data.europa.eu/doi/10.2785/321792. [Accessed 20 September 2024].
[45] Fan P, Song G, Zhai Z, Wu Y, Yu L. Fuel consumption estimation in heavy-duty trucks: integrating vehicle weight into deep-learning frameworks. Transp. Res. Part Transp Environ May 2024;130:104157. https://doi.org/10.1016/j.trd.2024.104157.
[46] Rahman SMA, Masjuki HH, Kalam MA, Abedin MJ, Sanjid A, Sajjad H. Impact of idling on fuel consumption and exhaust emissions and available idle-reduction technologies for diesel vehicles – a review. Energy Convers Manag Oct. 2013;74:171–82. https://doi.org/10.1016/j.enconman.2013.05.019.
[47] Eurostat. road_go_na_tgtt - national road transport by type of goods and type of transport (t, tkm) - annual data (from 2008 onwards). 2023. https://doi.org/10.2908/ROAD_GO_NA_TGTT.
[48] Crönert T, Minner S. Location selection for hydrogen fuel stations under emerging provider competition. Transport Res C Emerg Technol Dec. 2021;133:103426. https://doi.org/10.1016/j.trc.2021.103426.
[49] ETIS-BASE Consortium. Core database development for the European transport policy information system (ETIS). D9: final technical report v1 [Online]. Available: https://doi.org/10.3929/ethz-b-000023504; Jan. 2005.
[50] Szimba E, Kraft M, Ihrig J, Schimke A, Schnell O, Kawabata Y, Newton S, Breemersch T, Versteegh R, van Meijeren J, Jin-Xue H, de Stasio C, Fermi F. ETISplus database content and methodology: ETISplus deliverable D6. Project co-funded by the European commission under the 7th framework programme. 2013. https://doi.org/10.13140/RG.2.2.16768.25605.
[51] Eurostat, 'road_go_ta_tott - road freight transport by type of operation and type of transport (t, tkm, vehicle-km) - annual data'. doi: 10.2908/road_go_ta_tott.
[52] Speth D, Sauter V, Plötz P, Signer T. Synthetic European road freight transport flow data. Data Brief Feb. 2022;40:107786. https://doi.org/10.1016/j.dib.2021.107786.
[53] Eurostat, 'road_go_na_dctg - National road freight transport by distance class, type of goods and type of transport (t) - annual data (from 2008 onwards)'. doi: https://doi.org/10.2908/ROAD_GO_NA_DCTG.
[54] Copernicus, 'CORINE Land Cover 2018 (vector/raster 100 m), Europe, 6-yearly'. doi: https://doi.org/10.2909/71c95a07-e296-44fc-b22b-415f42acfdf0.
[55] European Commission, 'Trans-European transport network TENtec, annex I: maps of the comprehensive and core network'.
[56] QGIS Development Team, QGIS Geographic Information System. Open Source Geospatial Foundation Project. http://qgis.org. [Online]. Available: https://qgis.org/.
[57] Dijkstra EW. A note on two problems in connexion with graphs. Numer Math Dec. 1959;1(1):269–71. https://doi.org/10.1007/BF01386390.
[58] De Padova A, Schiera DS, Minuto FD, Lanzini A. Italian TEN-T road network and Hydrogen Refueling Station nodes, vol. 30. Zenodo; 2024. https://doi.org/10.5281/zenodo.13860416. Sep.
[59] Hart WE, et al. *Pyomo — optimization Modeling in Python*, vol. 67. In: Springer optimization and its applications. vol. 67. Cham: Springer International Publishing; 2017. https://doi.org/10.1007/978-3-319-58821-6.
[60] IBM ILOG CPLEX optimization studio [Online]. Available, https://www.ibm.com/docs/en/icos/www.ibm.com/docs/en/icos/22.1.1. [Accessed 12 July 2024].
[61] H2Mobility. Overview hydrogen refuelling for heavy duty vehicles [Online]. Available: https://h2-mobility.de/wp-content/uploads/sites/2/2021/08/H2-MOBILITY_Overview-Hydrogen-Refuelling-For-Heavy-Duty-Vehicles_2021-08-10.pdf; 2021.
[62] E. Mulholland, P.-L. Ragon, and F. Rodríguez, 'CO2 emissions from trucks in the European Union: an analysis of the 2020 reporting period'.
[63] ISPRA. Italian greenhouse gas inventory 1990-2022. National inventory report [Online]. Available: https://www.isprambiente.gov.it/files2024/pubblicazioni/rapporti/nir-2024-r-398-24.pdf. [Accessed 13 June 2024].
[64] Squadrito G, Maggio G, Nicita A. The green hydrogen revolution. Renew Energy Nov. 2023;216:119041. https://doi.org/10.1016/j.renene.2023.119041.
[65] Gestore dei Servizi Energetici S.p.A. (GSE). Rapporto statistico 2023 - solare fotovoltaico. 2024.
[66] Stolte M, Minuto FD, Lanzini A. Optimizing green hydrogen production from wind and solar for hard-to-abate industrial sectors across multiple sites in Europe. Int J Hydrogen Energy Aug. 2024;79:1201–14. https://doi.org/10.1016/j.ijhydene.2024.07.106.
[67] M. Giuli, 'Italy in the international hydrogen economy'.
[68] Guzzini A, Brunaccini G, Aloisio D, Pellegrini M, Saccani C, Sergi F. A new geographic information system (GIS) tool for hydrogen value chain planning optimization: application to Italian highways. Sustainability Jan. 2023;15(3):2080. https://doi.org/10.3390/su15032080.
[69] Gandiglio M, Marocco P. Mapping hydrogen initiatives in Italy: an overview of funding and projects. Energies Jan. 2024;17(11). https://doi.org/10.3390/en17112614. Art. no. 11.
[70] Novo R, Minuto FD, Bracco G, Mattiazzo G, Borchiellini R, Lanzini A. Supporting decarbonization strategies of local energy systems by de-risking investments in renewables: a case study on pantelleria island. Energies Feb. 2022;15(3):1103. https://doi.org/10.3390/en15031103.